symmetry

IMPACT FACTOR 2.2

CITESCORE 5.4

Article

Schwinger–Keldysh Path Integral Formalism for a Quenched Quantum Inverted Oscillator

Sayantan Choudhury, Suman Dey, Rakshit Mandish Gharat, Saptarshi Mandal and Nilesh Pandey

Special Issue
Symmetry: Feature Papers 2024

Edited by
Prof. Dr. Sergei Odintsov

MDPI

https://doi.org/10.3390/sym16101308

symmetry

MDPI

Article

Schwinger–Keldysh Path Integral Formalism for a Quenched Quantum Inverted Oscillator

Sayantan Choudhury [1,*], Suman Dey [2], Rakshit Mandish Gharat [3], Saptarshi Mandal [4] and Nilesh Pandey [1]

[1] Centre For Cosmology and Science Popularization (CCSP), SGT University, Gurugram 122505, Haryana, India; nilesh911999@gmail.com or nileshpandey_2k18ep053@dtu.ac.in
[2] Department of Physics, Visva-Bharati University, Santiniketan 731235, West Bengal, India; dey.suman.vbu@gmail.com or 03323081942@visva-bharati.ac.in
[3] Department of Physics, National Institute of Technology Karnataka, Surathkal 575025, Karnataka, India; rakshitmandishgharat.196ph018@nitk.edu.in
[4] Department of Physics, Indian Institute of Technology Kharagpur, Kharagpur 721302, West Bengal, India; saptarshijhikra@gmail.com or saptarshijhikra@kgpian.iitkgp.ac.in
* Correspondence: sayantan_ccsp@sgtuniversity.org or sayanphysicsisi@gmail.com

Abstract: In this work, we study the time-dependent behavior of quantum correlations of a system of an inverted oscillator governed by out-of-equilibrium dynamics using the well-known *Schwinger–Keldysh formalism* in the presence of quantum mechanical quench. Considering a generalized structure of a time-dependent Hamiltonian for an inverted oscillator system, we use the *invariant operator method* to obtain its eigenstate and continuous energy eigenvalues. Using the expression for the eigenstate, we further derive the most general expression for the generating function as well as the out-of-time-ordered correlators (OTOCs) for the given system using this formalism. Further, considering the time-dependent coupling and frequency of the quantum inverted oscillator characterized by quench parameters, we comment on the dynamical behavior, specifically the early, intermediate and late time-dependent features of the OTOC for the quenched quantum inverted oscillator. Next, we study a specific case, where the system of an inverted oscillator exhibits chaotic behavior by computing the *quantum Lyapunov exponent* from the time-dependent behavior of OTOCs in the presence of the given quench profile.

Keywords: quantum Mechanics, out-of-equilibrium physics, statistical mechanics, condensed Matter physics, non-equilibrium physics, quantum chaos.

Citation: Choudhury, S.; Dey, S.; Gharat, R.M.; Mandal, S.; Pandey, N. Schwinger–Keldysh Path Integral Formalism for a Quenched Quantum Inverted Oscillator. *Symmetry* **2024**, *16*, 1308. https://doi.org/10.3390/sym16101308

Academic Editors: Angel Gómez Nicola and Sergei Odintsov

Received: 10 August 2024
Revised: 26 September 2024
Accepted: 2 October 2024
Published: 3 October 2024

1. Introduction

In theoretical high-energy physics, the underlying concept of the Feynman path integral is applicable to quantum systems for which the vacuum state in the far future is exactly the same as in the far past. Clearly, the Feynman path integral is not applicable for quantum systems with a dynamical background. The Schwinger–Keldysh [1–5] formalism appears within the framework of quantum mechanics, where the physical system is placed on a dynamical background, i.e., quantum dynamics of the system is far from equilibrium. Schwinger–Keldysh formalism seems to be the most formidable choice to evaluate generating functionals and correlation functions in out-of-equilibrium quantum field theory and statistical mechanics [6]. It unravels the prodigious toolbox of equilibrium quantum field theory to out-of-equilibrium problems. There are large numbers of applications of out-of-equilibrium dynamics in various fields, for instance, condensed matter physics [7–11], cosmology [12–15] (in the context of the primordial universe), black hole physics [16,17], high-energy physics (theory and phenomenology) [18–22], and more.

The time-dependent states for dynamical quantum systems can be computed by solving the *Time-Dependent Schrödinger Equation* (TDSE). One of the ways to solve a TDSE is by constructing the *Lewis–Riesenfeld invariant operator* and this is often termed as an

invariant operator representation of the wavefunction [23]. Some works following this approach to compute the time-dependent eigenstates are reported in refs. [24–28].

The highly complex behavior of quantum systems can often be studied using a simple model of a Standard Harmonic Oscillator (SHO). The sister to the SHO is the inverted harmonic oscillator (IHO) that has remarkable properties which are applicable throughout many disciplines of physics [13,20,29–48]. The quantum treatment of the IHO is exactly solvable, similar to that of the SHO. Unlike the SHO, the IHO can be used to model complicated types of out-of-equilibrium systems.

A key idea for quantifying the propagation of detailed quantum correlation at out-of-equillbrium, information theoretic scrambling via exponential growth, and quantum chaos can be easily studied via out-of-time-ordered correlators or simply "OTOCs" [49]. OTOCs have been widely used as a tool to probe quantum chaos in quantum systems [50–57]. In a more general sense, an OTOC is a mathematical tool whereby one can easily quantify quantum mechanical correlations at out-of-equilibrium. Motivated by the work of [58], Kitaev [59] emphasized arbitrarily ordered 4-point correlation functions, as "out-of-time-ordered correlators", in constructing analogies between effective field theories, making the connection between superconductors [60] and black holes [61,62].

Most of the recent works in many-body physics focus on studying dynamics of quantum systems where some time-dependent parameter is varied suddenly or very slowly. This is commonly referred to as a quantum quench. The quench protocol is said to drive any out-of-equilibrium system and in turn can trigger the thermalization process of these systems, [63–65]. The effects of quenches in quantum systems have even been explored experimentally for cold atoms in [66–75]. A few of the works focusing on OTOCs in the context of quenched systems are [76–80].

Motivated by all these ideas, in this work, we compute an OTOC for inverted oscillators having a quenched coupling and frequency, using Schwinger–Keldysh path integral formalism. In Section 2, the continuous energy eigenvalues and normalized wavefunction for a generic Hamiltonian of a time-dependent inverted oscillator are computed [81] using the Lewis–Riesenfeld invariant method. In Section 3, we construct the action for the Lagrangian of a generic time-dependent inverted oscillator. Using this action, we derive the generating function for the inverted oscillator in Section 4. We modify this generating function using the Schwinger–Keldysh path integral formalism in Section 5, following the advice of [6]. Using this generating function and Green's functions computed in Appendix B, we finally compute the OTOC for inverted oscillators in terms of Green's functions in Section 6. In Section 7, we numerically study the dynamical behavior of the OTOC by quenching coupling and frequency of the inverted oscillator. We also compute the Lyapunov exponent and comment on the chaotic behavior of the inverted oscillator in this section. Section 8 serves as the final section of our study before providing pertinent future possibilities and directions.

2. Formulation of Time-Dependent Generalized Hamiltonian Dynamics

In this section, we explicitly discuss the crucial role of a system described by a time-dependent quantum mechanical inverted oscillator in a very generic way to deal with path integrals and different types of quantum correlation functions (anti-time-ordered, time-ordered, and out-of-time-ordered). A generalized Hamiltonian for a time-dependent inverted oscillator can be written as

$$\hat{H}(t) = \frac{1}{m(t)}\hat{p}^2 - \frac{1}{2}m(t)\Omega^2(t)\hat{q}^2 + \frac{1}{2}f(t)(\hat{p}\hat{q} + \hat{q}\hat{p}). \tag{1}$$

Here, $\hat{q}(t)$ denotes the time-dependent generalized coordinate, $m(t)$ is the time-dependent mass, $\Omega(t)$ is the time-dependent frequency, and $f(t)$ is a time-dependent coupling parameter. In general, these time-dependent parameters can be anything. It is significant to note that, in contrast to the SHO, the second term, which represents the potential energy of the inverted harmonic oscillator, has a negative sign. The main reason for the negative sign

in the potential energy is that for an inverted oscillator, the harmonic oscillator frequency, $\omega(t)$, is replaced by $i\omega(t)$. We can write the Euler–Lagrange equation for the coordinate $\hat{q}(t)$ of the inverted oscillator as

$$\left(\mathcal{D}_t - \Omega_{eff}^2\right)\hat{q}(t) = 0, \tag{2}$$

where the differential operator $\mathcal{D}_t$ is defined as

$$\mathcal{D}_t = \left(\frac{d^2}{dt^2} + \frac{d\ln m(t)}{dt}\frac{d}{dt}\right). \tag{3}$$

The squared effective time-dependent frequency in Equation (2) is defined by

$$\Omega_{eff}^2(t) = \Omega^2(t) + f^2(t) + \frac{\dot{m}(t)}{m(t)}f(t) + \dot{f}(t). \tag{4}$$

where the dot corresponds to the differentiation with respect to time "t". Then, the Euler–Lagrange equation in (3) gives the equation of motion in the simplified form as

$$\ddot{\hat{q}} + \frac{\dot{m}}{m}\dot{\hat{q}} - \Omega_{eff}^2(t)\hat{q} = 0. \tag{5}$$

Next, the TDSE for the abovementioned time-dependent system can then be written as

$$\hat{H}(t)\Psi(q,t) = i\frac{\partial\Psi(q,t)}{\partial t}. \tag{6}$$

Now, to derive the eigenstates and energy eigenvalues of the above TDSE, we will use the Lewis–Riesenfeld invariant operator method in the next section, which will be an extremely useful tool to deal with the rest of the problem.

Lewis–Riesenfeld Invariant Method

In this subsection, we apply the technique of the Lewis–Riesenfeld invariant operator to calculate the time-dependent eigenstates and energy eigenvalues for the generalized Hamiltonian of inverted oscillators as given in Equation (1).

The Lewis–Riesenfeld invariant method is advantageous for obtaining the complete solution of an inverted harmonic oscillator with a time-dependent frequency having $\mathcal{PT}$ symmetry. In this subsection, we will construct a dynamical invariant operator to transition the eigenstates of the Hamiltonian from the prescribed initial to final configurations in arbitrary time. Let us assume an invariant operator $\hat{I}(t)$, which is a hermitian operator and explicitly satisfies the relation

$$\frac{d\hat{I}(t)}{dt} = \frac{1}{i}[\hat{I}(t), \hat{H}(t)] + \frac{\partial\hat{I}(t)}{\partial t}, \tag{7}$$

so that its expectation values remain constant in time. Here, $\hat{H}(t)$ is the time-dependent Hamiltonian of our system defined earlier in Equation (1). If the exact form of the invariant operator, $\hat{I}(t)$, does not contain any time derivative operators, it allows one to write the solutions of the TDSE as

$$\psi_n(q,t) = e^{i\mu_n(t)}\varphi_n(q,t). \tag{8}$$

Here, $\varphi_n(q,t)$ is an eigenfunction of $\hat{I}(t)$ with eigenvalue n, and $\mu_n(t)$ is the time-dependent phase function. Note that for the sake of simplicity, we are writing $\hat{q}$ as q and the same for other operators. This means that we further remove all hats. Next, we consider a time-dependent linear invariant operator for the system in the form

$$I(t) = \alpha(t)q + K(t)p + \gamma(t), \tag{9}$$

where $\alpha(t)$, $K(t)$, and $\gamma(t)$ are the time-dependent real functions. Using Equation (7), we obtain

$$\begin{aligned} \dot{\alpha}(t) + \alpha(t)f(t) &= -K(t)m(t)\Omega^2(t) \\ \dot{K}(t) - K(t)f(t) &= -\frac{\alpha(t)}{m(t)} \\ \dot{\gamma}(t) &= 0. \end{aligned} \tag{10}$$

From Equation (10), one can find the following second-order differential equation:

$$\ddot{K} + \frac{\dot{m}}{m}\dot{K} - \Omega_{eff}^2(t)K = 0, \tag{11}$$

where the squared effective time-dependent frequency was defined in Equation (4) before. Therefore, we can write Equation (9) as

$$I(t) = K(t)p - m(t)\Big[\dot{K(t)} - K(t)f(t)\Big]q. \tag{12}$$

Now, we intend to find the eigenstate $\varphi_n(q,t)$ of $I(t)$ using the following eigenvalue equation:

$$I\varphi_n(q,t) = n\varphi_n(q,t) \tag{13}$$

Here, the eigenstates satisfy the orthonormalization condition, which is $\langle\varphi_n|\varphi_{n'}\rangle = \delta(n-n')$. Substituting the expression of $I(t)$ from Equation (12) in the above Equation (13), one can find the continuous eigenstates of the inverted oscillator:

$$\varphi_n = N\exp\left\{\frac{im(t)}{2K(t)}\left[[\dot{K}(t) - f(t)K(t)]q^2 + \frac{2n}{m(t)}q\right]\right\}. \tag{14}$$

It is very straightforward to calculate the normalizing constant, N, which is given by the following expression:

$$N = \sqrt{\frac{1}{2\pi K}}. \tag{15}$$

One can find the phase factor by inserting the eigenfunction of the invariant operator in TDSE and solving the following equation:

$$\dot{\mu}_n\varphi_n = \left(i\frac{\partial}{\partial t} - H\right)\varphi_n. \tag{16}$$

Using Equation (8), we can write the wavefunction in the following normalized form:

$$\psi_n = \sqrt{\frac{1}{2\pi K}}\, e^{i\mu_n(t)}\exp\left\{\frac{im(t)}{2K(t)}\left[[\dot{K}(t) - f(t)K(t)]q^2 + \frac{2n}{m(t)}q\right]\right\}. \tag{17}$$

Now, to prove that the wavefunctions are always finite, we have to find the integration over all possible continuous eigenvalues, which is given by

$$\Psi(q,t) = \int_{-\infty}^{\infty} g(n)\ \psi_n(q,t)\ dn. \tag{18}$$

Here, $g(n)$ is the weight function. It helps one to find which state the system is in. Let us consider the weight function as a Gaussian function, which is of the following exact form:

$$g(n) = \frac{\sqrt{a}}{(2\pi)^{\frac{1}{4}}}\exp\left(-\frac{a^2n^2}{4}\right). \tag{19}$$

Here, 'a' is a real positive constant. Substituting the above form of weight function in Equation (18) and integrating over all possible continuous eigenvalues, one can write the wavefunction for inverted oscillator as

$$\Psi(q,t) = \left(\frac{2A(t)}{\pi}\right)^{1/4} \exp\left\{iB_2(t) + [iB_1(t) - A(t)]q^2\right\}. \tag{20}$$

Here, we define the time-dependent functions as

$$\begin{aligned} A(t) &= \left[K^2a^2\left(1 - \frac{4y^2}{a^4}\right)\right]^{-1}, \\ B_1(t) &= \frac{m(\dot{K} - fK)}{2K} + \frac{2y}{K^2a^4\left(1 + \frac{4y^2}{a^4}\right)}, \\ B_2(t) &= \frac{1}{2}\tan^{-1}\frac{2y}{a^2}, \\ y(t) &= \int_0^t \frac{d\tau}{m(\tau)K^2(\tau)}. \end{aligned} \tag{21}$$

Now, having obtained the normalization factor, we can write the expression for the energy of our desired quantum system as

$$E = \sqrt{\frac{2A(t)}{\pi}} \int_{-\infty}^{\infty} \Psi^* \hat{H} \Psi \, dq. \tag{22}$$

By inserting Equation (20), $\hat{H}$ and conjugate of Equation (20) into Equation (22), one can show that the time-dependent energy for an inverted oscillator is given by the following expression:

$$E = \frac{1}{2m(t)}\left(\frac{B_1^2(t)}{A(t)} + A(t)\right) + \frac{1}{8}\frac{m(t)\Omega^2(t)}{A(t)} + \frac{f(t)B_1(t)}{2A(t)}. \tag{23}$$

It is interesting to observe that the energy eigenvalues are independent of n but energy is a continuous function of time. Furthermore, there is no zero-point energy associated with this system of inverted oscillator.

3. Evaluation of Action

In this section, we start with a Lagrangian of the inverted oscillator and derive the representative action for the generalized inverted oscillator. We express the action in terms of Green's functions, which are derived in Appendix B. The action thus obtained will be useful for deriving the generating function of inverted oscillator. Here, it is important to note that the generating function in the present context physically represents the partition function in an Euclidean signature.

As Green's function for inverted oscillator given in Equation (A18) is hyperbolic in nature, one can use the hyperbolic identities. Inferring from [6], one can then write the classical field solution for the inverted oscillator as

$$\bar{q}(t) = \frac{1}{G(T)}\left\{q_f G(t - t_0) + q_0\, G(t_f - t) + \int_{t_0}^{t_f} dt' \Big[G(T)\Theta(t - t')G(t - t') - G(t - t_0)G(t_f - t')\Big] J(t')\right\}. \tag{24}$$

The time derivative of this field can be given by

$$\dot{\bar{q}} = \frac{1}{G(T)}\left[q_f \dot{G}(t - t_0) - q_0\dot{G}(t - t_f) + \int_{t_0}^{t_f} dt'[G(T)\Theta(t - t')\dot{G}(t - t') - \dot{G}(t - t_0)G(t_f - t')]J(t')\right]. \tag{25}$$

Here, $T \equiv t_f - t_0$, such that t_0 and t_f denote the initial time and final time, respectively. Also, $\bar{q}(t_0) = q_0$ and $\bar{q}(t_f) = q_f$ are the initial and final field configurations, respectively. Applying the boundary condition $\dot{G}(0) = 1$, one can find

$$\dot{\bar{q}}(t_0) = \frac{1}{G(T)}\left[q_f - q_0\dot{G}(T) - \int_{t_0}^{t_f} dt'\, G(t_f - t')J(t')\right]. \tag{26}$$

Furthermore, using the hyperbolic identity,

$$\dot{G}(T)G(t_f - t) - \dot{G}(T)G(t_f - t) = G(t - t_0), \tag{27}$$

we obtain

$$\dot{\bar{q}}(t_f) = \frac{1}{G(T)}\left[q_f\dot{G}(T) - q_0 + \int_{t_0}^{t_f} dt'\, G(t' - t_0)J(t')\right] \tag{28}$$

In general, the action for any field is given by

$$S = \int_{t_0}^{t_f} [\mathcal{L} + J(t)q(t)]dt. \tag{29}$$

Here, the term $J(t)$ is an auxiliary time-dependent field and $\mathcal{L}$ is the Lagrangian of the system. For an inverted oscillator, the representative Lagrangian can be written as

$$\mathcal{L} = \frac{1}{2}m(t)\dot{q}^2 + m(t)\omega(t)^2q^2 - f(t)m(t)\dot{q}q \tag{30}$$

Substituting Equation (30) with the Euler–Lagrange equation, the equation of motion for the inverted oscillator then becomes,

$$m(t)\ddot{q} + \dot{m(t)}\dot{q} - \left[m(t)\omega(t)^2 - f(t)\dot{m(t)} - m(t)\dot{f(t)}\right]q = 0 \tag{31}$$

Substituting Equation (30) in (29), the action for the inverted oscillator can be expressed as

$$S = \int_{t_0}^{t_f}\left[\left(\frac{1}{2}m(t)\dot{q}^2 + \frac{1}{2}m(t)\omega^2(t)q^2 - f(t)m(t)\dot{q}q\right) + J(t)q(t)\right]dt. \tag{32}$$

Using the equation of motion, i.e., Equation (31) and the definition of classical field solution as stated in Equation (24), we find the classical limit for the action of inverted oscillator as

$$S_{cl}(q_0, q_f|J) \equiv S(\bar{q}) = \frac{1}{2}m(t)\bar{q}\dot{\bar{q}}\Big|_{t_0}^{t_f} - \frac{1}{2}f(t)m(t)\bar{q}^2\Big|_{t_0}^{t_f} + \frac{1}{2}\int_{t_0}^{t_f} dtJ(t)\bar{q}(t). \tag{33}$$

The final expression for the action can be obtained using Equation (26) and Equation (28), as given below:

$$\begin{aligned} S(q_0, q_f|J) = \frac{1}{2}\Bigg[m(t_f)\frac{1}{G(T)}\Bigg\{q_f^2\dot{G}(T) - q_0q_f + \int_{t_0}^{t_f} dt' q_f G(t' - t_0)J(t')\Bigg\} - m(t_0)\frac{1}{G(T)}\Bigg\{q_fq_0 - q_0^2\dot{G}(T) + \\ \int_{t_0}^{t_f} dt' q_0 G(t_f - t')J(t')\Bigg\}\Bigg] - \frac{1}{2}\left[f(t_f)m(t_f)q_f^2 - f(t_0)m(t_0)q_0^2\right] + \frac{1}{2}\Bigg\{\frac{1}{G(T)}\int_{t_0}^{t_f} dt[G(t - t_0)q_f + G(t_f - t)q_0]J(t) \\ - \frac{1}{G(T)}\int_{t_0}^{t_f} dt\int_{t_0}^{t_f} dt'\,[\Theta(t - t')G(t_f - t)G(t' - t_0) + \Theta(t' - t)G(t_f - t')G(t - t_0)]J(t)J(t')\Bigg\}. \end{aligned} \tag{34}$$

4. Generating Function

In this section, the prime objective is to derive the expression for the generating function for the time-dependent inverted oscillator, using the action that we computed in

the previous section.
The generating function for a particular classical action is given by

$$Z(q_0, t_0; q_f, t_f|J) = C(T) \exp\Big(iS_{cl}(q_0, t_0; q_f|J)\Big), \tag{35}$$

where $T = t_f - t_0$, and $C(T)$ is an overall factor that does not depend on the external source J. Hence, we can rewrite

$$Z(q_0, t_0; q_f, t_f) := Z(q_0, t_0; q_f, t_f|0) = C(T) \exp\Big(iS_{cl}(q_0, t_0; q_f, t_f|0)\Big). \tag{36}$$

The generating function without the source, i.e., $Z(q_0, t_0; q_f, t_f)$ can be represented by the transition amplitude $\langle q_f| e^{i\hat{H}T} |q_0\rangle$ and can even be decomposed, as shown below:

$$\begin{aligned} Z(q_0, t_0; q_2, t_2) = \langle q_2| e^{-it_2\hat{H}} e^{it_0\hat{H}} |q_0\rangle &= \langle q_2| e^{-it_2\hat{H}} e^{it_1\hat{H}} e^{-it_1\hat{H}} e^{it_0\hat{H}} |q_0\rangle \\ &= \int_{-\infty}^{\infty} dq_1 \langle q_2| e^{-it_2\hat{H}} e^{it_1\hat{H}} |q_1\rangle \langle q_1| e^{-it_1\hat{H}} e^{it_0\hat{H}} |q_0\rangle \\ &= \int_{-\infty}^{\infty} dq_1 Z(q_1, t_1; q_2 t_2|0) Z(q_0, t_0; q_1, t_1|0) \end{aligned} \tag{37}$$

Applying the composition law shown in Equation (37), we can rewrite Equation (35) as

$$\int_{-\infty}^{\infty} dq_1 Z(q_1, t_1; q_2 t_2|0) Z(q_0, t_0; q_1, t_1|0) = C(t_1 - t_0) C(t_2 - t_1) e^{i(S_{cl}(q_0, t_0; q_1, t_1) + S_{cl}(q_1, t_1; q_2, t_2))} \tag{38}$$

From Equation (34), we can write the action as

$$S_{cl}(q_0, t_0; q_f, t_f|0) = \frac{\dot{G}(t_f - t_0)\Big[(m(t_f)q_f^2 + m(t_0)q_0^2\Big] - \Big[m(t_f) + m(t_0)\Big] q_f q_0}{2G(t_f - t_0)} - \frac{1}{2}\Big[f(t_f)m(t_f)q_f^2 - f(t_0)m(t_0)q_0^2\Big]. \tag{39}$$

If one considers that the system undergoes a quantum dynamical event from q_0 to q_1 and q_1 to q_2, one can use Equation (39) to find the sum of actions obtained from the classical solution. It can then be shown that

$$S_{cl}(q_0, t_0; q_1, t_1|0) + S_{cl}(q_1, t_1; q_2, t_2|0) = \frac{N}{2G(t_1 - t_0)G(t_2 - t_1)} - \frac{1}{2}\Big[f(t_2)m(t_2)q_2^2 - f(t_0)m(t_0)q_0^2\Big], \tag{40}$$

where the normalization factor N is given by the following expression:

$$\begin{aligned} N = {} & G(t_2 - t_0)q_1^2 + G(t_2 - t_1)\dot{G}(t_1 - t_0)m(t_0)q_0^2 + G(t_1 - t_0)\dot{G}(t_2 - t_0)m(t_2)q_2^2 \\ & - q_1\Big\{[m(t_1) + m(t_0)]q_0 G(t_2 - t_1) + [m(t_1) + m(t_2]q_2 G(t_1 - t_0)\Big\}. \end{aligned} \tag{41}$$

Using algebraic manipulation, one can rewrite the expression for the normalization factor N as

$$\begin{aligned} N = {} & G(t_2 - t_0)m(t_1)\left[q_1 - \frac{2q_1[m(t_1) + m(t_0)]G(t_2 - t_1)q_0 + [m(t_2) + m(t_1)]q_2 G(t_1 - t_0)}{2m(t_1)G(t_2 - t_0)}\right]^2 + G(t_2 - t_1)\dot{G}(t_1 - t_0)m(t_0)q_0^2 \\ & + G(t_1 - t_0)\dot{G}(t_2 - t_1)m(t_2)q_2^2 - \frac{\Big[[m(t_1) + m(t_0)]G(t_2 - t_1)q_0 + [m(t_2) + m(t_1)G(t_1 - t_0)\Big]^2}{2m(t_1)G(t_2 - t_0)}. \end{aligned} \tag{42}$$

Note that to avoid long equations, henceforth, we denote

$$\left[q_1 - \frac{2q_1[m(t_1)+m(t_0)]G(t_2-t_1)q_0 + [m(t_2)+m(t_1)]q_2G(t_1-t_0)}{2m(t_1)G(t_2-t_0)}\right]^2 \equiv \left(q_1\ldots\right)^2$$

To find the generating function using Equation (38), one needs to evaluate integration over q_1. We therefore rearrange the terms in the above equation as follows:

$$\begin{aligned}
&N - G(t_2-t_1)m(t_1)(q_1\ldots)^2 = \\
&\tfrac{1}{2m(t_1)G(t_2-t_0)}\Big(2m(t_0)m(t_1)G(t_2-t_0)G(t_2-t_1)\dot{G}(t_1-t_0)q_0^2 + 2m(t_1)m(t_2)G(t_1-t_0)\dot{G}(t_2-t_1)G(t_2-t_0)q_2^2 \\
&-m^2(t_1)G^2(t_2-t_1)q_0^2 - 2m(t_1)m(t_0)G^2(t_2-t_1)q_0^2 - m^2(t_0)G(t_2-t_1)q_0^2 - m^2(t_2)G^2(t_1-t_2)q_2^2 \\
&-2m(t_2)m(t_1)G^2(t_1-t_0)q_2^2 - m^2(t_1)G^2(t_1-t_0)q_2^2 - 2q_0q_2G(t_1-t_0)G(t_2-t_1)[m(t_1)+m(t_0)][m(t_2)+m(t_1)]\Big).
\end{aligned} \tag{43}$$

The hyperbolic relations in terms of Green's function and its time derivatives are given below:

$$\begin{aligned}
G(t_2-t_0)\dot{G}(t_1-t_0) - G(t_2-t_1) &= \dot{G}(t_2-t_0)G(t_1-t_0) \\
G(t_2-t_0)\dot{G}(t_2-t_1) - G(t_1-t_0) &= \dot{G}(t_2-t_0)G(t_2-t_1).
\end{aligned} \tag{44}$$

Using these hyperbolic relations, one can further simplify Equation (43) and write it in the present form:

$$\begin{aligned}
&N - G(t_2-t_1)m(t_1)\left(q_1\ldots\right)^2 = \tfrac{1}{2m(t_1)G(t_2-t_0)}\Big\{2m(t_0)m(t_1)G(t_2-t_1)\dot{G}(t_2-t_0)G(t_1-t_0)q_0^2 \\
&+2m(t_1)m(t_2)G(t_1-t_0)\dot{G}(t_2-t_0)G(t_2-t_1)q_2^2 - [m^2(t_1)+m^2(t_0)]G^2(t_2-t_1)q_0^2 \\
&-[m^2(t_1)+m^2(t_2)]G^2(t_1-t_0)q_2^2 - 2q_0q_2G(t_1-t_0)G(t_2-t_1)[m(t_1)+m(t_0)][m(t_2)+m(t_1)]\Big\}.
\end{aligned} \tag{45}$$

Using the above expression, the sum of classical actions in Equation (40) can be simplified to the following form:

$$\begin{aligned}
&S_{cl}(q_0,t_0;q_1,t_1|0) + S_{cl}(q_1,t_1;q_2,t_2|0) = \\
&\qquad S_{cl}(q_0,t_0;q_2,t_2|0) + \frac{G(t_2-t_0)m(t_1)}{2G(t_1-t_0)G(t_2-t_1)}\left[q_1-\ldots\right]^2 + \frac{q_2q_0}{2G(t_2-t_0)}\left[m(t_1)\frac{m(t_0)m(t_2)}{m(t_1)}\right] \\
&\qquad\qquad - \frac{\left\{\left[\frac{m^2(t_1)+m^2(t_0)}{m(t_1)}\right]G^2(t_2-t_1)q_0^2 + \left[\frac{m^2(t_1)+m^2(t_2)}{m(t_1)}\right]G^2(t_1-t_0)q_2^2\right\}}{4G(t_2-t_1)G(t_1-t_0)G(t_2-t_0)}.
\end{aligned} \tag{46}$$

The generating function of Equation (38) can then be evaluated as

$$Z(q_2,t_2;q_0,t_0|0) = C(t_1-t_0)C(t_2-t_1)e^{iS_{cl}(q_0,t_0;q_2,t_2|0)}\exp\left(\mathcal{R}\right)\int_{-\infty}^{\infty}dq_1\exp\left[\frac{iG(t_2-t_0)m(t_1)}{2G(t_1-t_0)G(t_2-t_1)}\left\{q_1^2-\ldots\right\}\right]. \tag{47}$$

Here, the factor $\mathcal{R}$ in the exponent is given by

$$\mathcal{R} = \left[i\left\{\frac{q_0q_2\left[m(t_1) - \frac{m(t_0)m(t_1)}{m(t_1)}\right]}{2G(t_2-t_0)} - \frac{\left\{\left[\frac{m^2(t_1)+m^2(t_0)}{m(t_1)}\right]G^2(t_2-t_1)q_0^2 + \left[\frac{m^2(t_1)+m^2(t_2}{m(t_1)}\right]G^2(t_1-t_0)q_2^2\right\}}{4G(t_2-t_1)G(t_1-t_0)G(t_2-t_0)}\right\}\right]. \tag{48}$$

Solving the integral over q_1 in Equation (47), we obtain

$$Z(q_2,t_2;q_0,t_0|0) = C(t_1-t_0)C(t_2-t_1)e^{iS_{cl}(q_2,t_2;q_0,t_0|0)}\exp(\mathcal{R})\sqrt{\frac{2\pi iG(t_2-t_1)G(t_1-t_2)}{G(t_2-t_0)m(t_1)}}. \tag{49}$$

Using Equation (36), one can evaluate the LHS of the above equation, and hence, we write

$$C(t_2-t_0)e^{iS_{cl}(q_2,t_2;q_0,t_0|0)} = C(t_1-t_0)C(t_2-t_1)e^{iS_{cl}(q_2,t_2;q_0,t_0|0)}\exp(\mathcal{R})\sqrt{\frac{2\pi iG(t_2-t_1)G(t_1-t_2)}{G(t_2-t_0)m(t_1)}}. \tag{50}$$

From the above equation, we can easily find

$$C(T) = \exp(-\mathcal{R})\sqrt{\frac{m(t_1)}{2\pi iG(T)}} \tag{51}$$

where $G(T) = G(t_f - t_0)$ is Green's function. Finally, substituting Equation (51) in Equation (47), the final expression for the generating function of the inverted oscillator is

$$Z(q_2,t_2;q_0,t_0|0) = \frac{\sqrt{m(t_1)}}{\sqrt{2\pi iG(T)}}\exp\left[i\left\{-q_1q_2\frac{\left\{m(t_1)-\frac{m(t_0)m(t_2)}{m(t_1)}\right\}}{2G(t_2-t_0)} + \frac{\left\{\left[\frac{m^2(t_1)+m^2(t_0)}{m(t_1)}\right]G^2(t_2-t_1)q_0^2 + \left[\frac{m^2(t_1)+m^2(t_2)}{m(t_1)}\right]G^2(t_1-t_0)q_2^2\right\}}{4G(t_2-t_1)G(t_1-t_0)G(t_2-t_0)}\right\}\right]e^{iS_{cl}(q_2,t_2;q_0,t_0|0)}. \tag{52}$$

5. Schwinger–Keldysh Path Integral

In this section, we give a brief idea of how the Feynman path integral leads to the Schwinger–Keldysh path integral for non-equilibrium systems. Moreover, we study in detail the generating function using the Schwinger–Keldysh path integral for inverted oscillators. Note that we follow the advice given in ref. [6] for an easy comparison.

The propagation function or generating function of a Feynman path integral can be expressed as

$$Z(q_0,t_0;q,t|0) = \int_{q(t_0)=q_0}^{q(t)=q}\mathcal{D}q(\cdot)\, e^{\int_{t_0}^{t}\mathcal{L}(q(t'))\,dt'}. \tag{53}$$

In Feynman's path integral formalism, one can calculate the moments of distribution by introducing an auxiliary variable (J) and taking the derivative of the generating function with respect to J. The one-point amplitude is then given by

$$\langle q_f|\, e^{-i\hat{H}t_f}\hat{q}(t_1)e^{i\hat{H}t_0}\,|q_0\rangle = -i\frac{\delta}{\delta J(t_1)}Z(q_0,q_f|J)\bigg|_{J=0}. \tag{54}$$

For multiple-field configurations, $Z(q_0,q_f|J)$ could generate the amplitude of time-ordered products of fields:

$$\langle q_f|\, e^{-i\hat{H}t_f}\mathcal{T}(\hat{q}(t_1)\ldots\hat{q}(t_n)e^{i\hat{H}t_0}\,|q_0\rangle = (-i)^n\frac{\delta^n}{\delta J(t_1)\ldots\delta J(t_n)}Z(q_0,q_f|J)\bigg|_{J=0}. \tag{55}$$

Here, $\mathcal{T}$ represents the time-ordering symbol. For out-of-equilibrium systems like the inverted oscillator, although we need to compute such correlators, we cannot use time-ordering and hence must use some other kind of formalism. The Schwinger–Keldysh contour facilitates refining to a time-folded contour and hence provides a path integral representation of the out-of-time-ordered correlators. In Figure 1, the four legs are denoted by each time stamp t_1, t_2, t_3, t_4 and we have taken the past-turning point in the contour at

time t_1 and future-turning point at certain time t. Now, for the action of an operator, e.g., θ at t_0, at a later time $t_1 > t_0$, it must be related by the usual Heisenberg evolution with unitary time evolution operator $U(t, t_0)$, i.e.,

$$\theta(t) = U(t, t_0)\theta(t_0)U^{\dagger}(t, t_0). \tag{56}$$

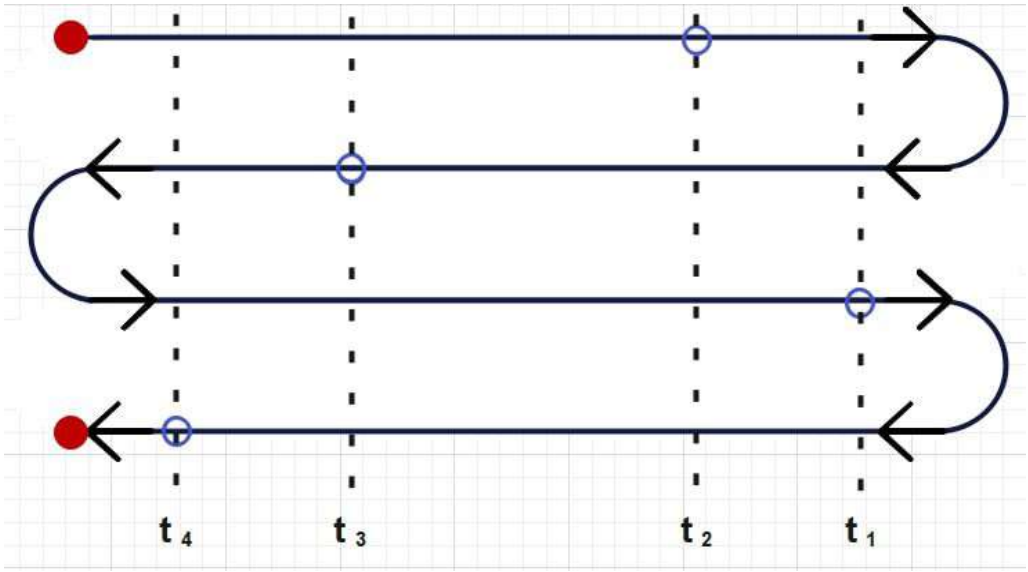

Figure 1. A schematic representation of Schwinger–Keldysh contour for the correlator functions with temporal ordering.

The source-free Feynman path integral is nothing but an evolution operator and it is related to the Schrödinger picture wavefunction if $\psi(q) = \langle q|\psi\rangle$. Thus, we can write

$$\Psi(q,t) = \int_{-\infty}^{\infty} dq_0 \langle q|\hat{U}(t-t_0)|q_0\rangle\langle q_0|\psi\rangle = \int_{-\infty}^{\infty} dq_0\, \psi(q_0) \int_{q_0}^{q_t} \mathcal{D}q(\cdot) e^{\int_{t_0}^{t} dt'\, \mathcal{L}(q(t'))}. \tag{57}$$

Note that the transportation event can be written as $\langle q|\, U(t-t_0)\, |q_0\rangle$; this mathematical expression tells us the history of propagation event from q_0 to q.

When we consider a special case that the wave density matrix $\hat{\rho} = |q_0\rangle\, \langle q_0|$ (ground state) is a pure state with definite coordinates, then the one-point correlator can be written as

$$\mathcal{T}(\hat{q}(t_1)\, e^{i\hat{H}t_0}\, \hat{\rho}\, e^{-i\hat{H}t_0}) = \langle q_0|\, e^{-i\hat{H}t_0} \hat{q}(t_1)\, e^{i\hat{H}t_0}\, |q_0\rangle\,. \tag{58}$$

On rewriting the above equation by introducing the identity operator $\hat{\rho}$, we can write the one-point correlator as

$$\mathcal{T}(\hat{q}(t_1)\, e^{i\hat{H}t_0}\, \hat{\rho}\, e^{-i\hat{H}t_0}) = \int_{-\infty}^{\infty} dq_f \int_{-\infty}^{\infty} dq_0 \int_{-\infty}^{\infty} dq_0' \,\langle q_f|\, e^{-i\hat{H}t_f} \hat{q}(t_1)\, e^{i\hat{H}t_0}\, |q_0\rangle\, \langle q_0|\, \hat{\rho}\, |q_0'\rangle\, \langle q_0'|\, e^{-i\hat{H}t_0}\, e^{i\hat{H}t_f}\, |q_f\rangle\,. \tag{59}$$

Using Equation (54), one can then write

$$\mathcal{T}(\hat{q}(t_1)\, e^{i\hat{H}t_0}\, \hat{\rho}\, e^{-i\hat{H}t_0}) = (-i)\frac{\delta}{\delta J(t_1)} \int_{-\infty}^{\infty} dq_f \int_{-\infty}^{\infty} dq_0 \int_{-\infty}^{\infty} dq_0'\, \rho(q_0, q_0')\, Z(q_0, q_f|J) Z(q_0', q_f|J')^* \Big|_{J=J'=0}. \tag{60}$$

Hence, we can define the generating function corresponding to the Schwinger–Keldysh path integral by comparing the above equation with Equation (58) as

$$Z(J, J') = \int_{-\infty}^{\infty} dq_f \int_{-\infty}^{\infty} dq_0 \int_{-\infty}^{\infty} dq_0'\, \rho(q_0, q_0')\, Z(q_0, q_f|J) Z(q_0', q_f|J')^*. \tag{61}$$

In Equation (61), if the state is pure, i.e., $\hat{\rho} = |\psi\rangle\langle\psi|$, then we can factorize the double integral over q_0, that is, the initial field configuration, as shown below:

$$\int_{-\infty}^{\infty} dq_0 \int_{-\infty}^{\infty} dq_0' \, \rho(q_0, q_0') \, Z(q_0, q_f|J) Z(q_0', q_f|J')^* = \left(\int_{-\infty}^{\infty} dq_0 \, \langle q_0|\psi\rangle Z(q_0, q_f|J) \right) \left(\int_{-\infty}^{\infty} dq_0' \, \langle q_0'|\psi\rangle \, Z(q_0', q_0|J') \right)^* \tag{62}$$

One can rewrite the above equation as

$$\int_{-\infty}^{\infty} dq_0 \int_{-\infty}^{\infty} dq_0' \, \rho(q_0, q_0') \, Z(q_0, q_f|J) Z(q_0', q_f|J')^* = \Psi(q_f|J)\Psi(q_f|J')^*, \tag{63}$$

where we define

$$\Psi(q_f|J) = \int_{-\infty}^{\infty} dq_0 \, \langle q_0|0\rangle \, Z(q_0, q_f|J). \tag{64}$$

Now, by using the wavefunction (18) for the ground state of the inverted oscillator given by

$$\langle q|0\rangle = \frac{\sqrt{a}}{(2\pi)^{\frac{1}{4}}} \left(\frac{1}{2\pi K(t)} \right)^{\frac{1}{2}} e^{\frac{-q^2}{2x_0^2}}, \tag{65}$$

and the density matrix $\hat{\rho} = |0\rangle\langle 0|$, we can express the generating function in its factorized form:

$$Z(J, J') = \int_{-\infty}^{\infty} dq_f \, \Psi(q_f|J)\Psi(q_f|J')^*. \tag{66}$$

Next, by using the equation for classical solution for the action given in Equation (34), we can write

$$\begin{aligned} \Psi(q_f|J) = \frac{\sqrt{a}}{(2\pi)^{\frac{1}{4}}} \left(\frac{1}{2\pi K(t)} \right)^{\frac{1}{2}} \frac{\sqrt{m(t_1)}}{\sqrt{2\pi G(T)}} \exp \Bigg[\frac{i}{2G(T)} \Bigg[& m(t_f)\dot{G}(T) q_f^2 - G(T) f(t_f) m(t_f) q_f^2 \\ & + \frac{\left[\frac{m^2(t_1) + m^2(t_f)}{m(t_1)} \right] G(t_1 - t_0) q_f^2}{2G(t_f - t_1)} + [m(t_f) + 1] \int_{t_0}^{t_f} dt' q_f G(t' - t_0) J(t') \\ & - 2 \int_{t_0}^{t_f} dt \int_{t_0}^{t_f} dt' \Theta(t - t') G(t_f - t') G(t' - t_0) \Bigg] J(t) J(t') \Bigg] \chi(q_f|J). \end{aligned} \tag{67}$$

Here, $\chi(q_f|J)$ denotes the contribution of integration over the initial field configuration, i.e., q_0. We compute this integral's contribution in Appendix A. Inserting Equation (A6) in Equation (67), one can show that

$$\begin{aligned} \Psi(q_f|J) = \frac{\sqrt{a}}{(2\pi)^{\frac{1}{4}}} \left(\frac{1}{2\pi K(t)} \right)^{\frac{1}{2}} \frac{\sqrt{m(t_1)}}{\sqrt{2\pi G(T)}} \sqrt{2\pi i G(T) \mathcal{A}^{-1}(t)} \exp \Bigg[\frac{i}{2G(T)} \Bigg\{ & m(t_f)\dot{G}(T) q_f^2 - G(T) f(t_f) m(t_f) q_f^2 \\ & + \frac{\left[\frac{m^2(t_1) + m^2(t_f)}{m(t_1)} \right] G(t_1 - t_0) q_f^2}{2G(t_f - t_1)} + [m(t_f) + 1] \int_{t_0}^{t_f} dt' \, q_f G(t_1 - t_0) J(t') \\ & - 2 \int_{t_0}^{t_f} dt \int_{t_0}^{t_f} dt' [\Theta(t - t') G(t_f - t') G(t' - t_0)] J(t) J(t') \Bigg\} \Bigg] \exp \Bigg[\frac{-i\mathcal{A}^{-1}(t)}{8G(T)} \times \\ & \left[\left\{ m(t_f) + m(t_0) + m(t_1) - \frac{m(t_0) m(t_f)}{m(t_1)} \right\} q_f - [m(t_0) + 1] \int_{t_0}^{t_f} dt \, G(t_f - t) J(t) \right]^2 \Bigg]. \end{aligned} \tag{68}$$

By performing similar steps, one can find $\Psi^*(q_f|J')$.

Substituting Equation (68) in Equation (66), one can write the generating function as

$$Z(J,J') = m(t_1)\frac{a}{\sqrt{2\pi}}\frac{\mathcal{A}^{-1}(t)}{2\pi K(t)}\exp\left[\frac{i}{2G(T)}[m(t_f)+1]\int_{t_0}^{t_f}dt'\, q_f G(t_1-t_0)[J(t')-J'(t')]\right.$$
$$\left.+2\int_{t_0}^{t_f}dt\int_{t_0}^{t_f}dt'[\Theta(t-t')G(t_f-t')G(t'-t_0)][J'(t)J'(t')-J(t)J(t')]\right]\int_{-\infty}^{\infty}dq_f\exp\left\{\mathcal{I}(J,J')\right\}. \tag{69}$$

Here, $\mathcal{I}(J,J')$ contains the terms having the contribution of the final field configuration, q_f, given by

$$\mathcal{I}(J,J') = \left[\frac{i\mathcal{A}^{-1}(t)}{8G(T)}\left(\left\{m(t_f)+m(t_0)+[m(t_1)-\frac{m(t_0)m(t_f)}{m(t_1)}\right\}q_f-[m(t_0)+1]\int_{t_0}^{t_f}dt\; G(t_f-t)J(t)\right)^2\right]$$
$$+\left[\frac{-i\mathcal{A}^{-1}(t)}{8G(T)}\left(\left\{m(t_f)+m(t_0)+[m(t_1)-\frac{m(t_0)m(t_f)}{m(t_1)}\right\}q_f-[m(t_0)+1]\int_{t_0}^{t_f}dt\; G(t_f-t)J(t)\right)^2\right]. \tag{70}$$

Since $\mathcal{A}^{-1}(t)$, as given in Equation (A2), is real, the q_f^2 terms in Equation (70) will be canceled out and the only term that contains q_f will be considered for the integration over the final configuration. The expression of $\mathcal{I}(J,J')$ upon simplification is then given by

$$\mathcal{I}(J,J') = \frac{4i\mathcal{A}^{-1}(t)}{8G(T)}\left[-q_f\frac{[m(t_0)+1]}{2}\left[m(t_f)+m(t_0)+m(t_1)-\frac{m(t_0)m(t_f)}{m(t_1)}\right]\left\{\int_{t_0}^{t_f}dt'G(t_f-t')[J'(t')-J(t)]\right\}\right.$$
$$\left.-\left[\frac{[m(t_0)+1]}{2}\int_{t_0}^{t_f}dt'G(t_f-t')J(t')\right]^2+\left[\frac{[m(t_0)+1]}{2}\int_{t_0}^{t_f}dt'G(t_f-t')J'(t')\right]^2\right] \tag{71}$$

We write the particular term of Equation (71) as

$$\mathcal{A}^{-1}(t)\left[\frac{[m(t_0)+1]}{2}\int_{t_0}^{t_f}dt'G(t_f-t')J(t')\right]^2=\mathcal{A}^{-1}(t)\frac{[m(t_0)+1]^2}{4}\int_{t_0}^{t_f}dt\int_{t_0}^{t_f}dt'G(t_f-t')G(t_f-t)J(t)J(t'). \tag{72}$$

Now, putting Equation (72) back into Equation (71), and then using the final expression of $\mathcal{I}(J,J')$ in Equation (69), we can write the generating function for the inverted oscillator as

$$Z(J,J') = m(t_1)\tfrac{a}{\sqrt{2\pi}}\tfrac{1}{2\pi K(t)}\tfrac{1}{|\mathcal{A}(t)|}\exp\left[\tfrac{i}{G(T)}\int_{t_0}^{t_f}dt\int_{t_0}^{t_f}dt'[\Theta(t-t')G(t_f-t)G(t'-t_0)][J'(t)J'(t')-J(t)J(t')]\right]$$
$$\times\int_{-\infty}^{\infty}dq_f\exp\left[\tfrac{i\mathcal{A}^{-1}(t)}{2G(T)}\left\{\tfrac{[m(t_0)+1]}{2}\left[m(t_f)+m(t_0)+m(t_1)-\tfrac{m(t_0)m(t_f)}{m(t_1)}\right]\left\{\int_{t_0}^{t_f}dt'G(t_f-t')[J(t')-J'(t')]\right\}q_f\right.\right.$$
$$\left.\left.+\tfrac{[m(t_0)+1]^2}{4}\left[\int_{t_0}^{t_f}dt\int_{t_0}^{t_f}dt'G(t_f-t')G(t_f-t)[J'(t)J'(t')-J(t)J(t')]\right]+[m(t_f)+1]\mathcal{A}(t)\int_{t_0}^{t_f}dt'q_fG(t'-t_0)\right.\right.$$
$$\left.\left.\times[J(t')-J'(t')]\right\}\right]. \tag{73}$$

Next, we define

$$j=\frac{[m(t_0)+1]}{2}\left[m(t_f)+m(t_0)+m(t_1)-\frac{m(t_0)m(t_f)}{m(t_1)}\right]\int_{t_0}^{t_f}dt'\left[G(t_f-t')[J'(t')-J(t)]\right]$$
$$+[m(t_f+1]\mathcal{A}(t)\int_{t_0}^{t_f}dt'\;G(t'-t_0)[J(t')-J'(t')]. \tag{74}$$

Then, the integral over the final field configuration in Equation (73) can be evaluated as

$$\int_{-\infty}^{\infty}\exp\left(\frac{i\mathcal{A}^{-1}(t)}{2G(t)}jq_f\right)dq_f=4\pi G(T)\mathcal{A}(t)\delta(j). \tag{75}$$

.

Finally, the generating function can be written as

$$Z(J,J') = \frac{2m(t_1)aG(T)}{\sqrt{2\pi K(t)}}\,\delta\Bigg(\int_{t_0}^{t_f} dt'[m(t_f)+1]\mathcal{A}(t)G(t'-t_0) + \frac{[m(t_0)+1]}{2}\left[m(t_f)+m(t_0)+m(t_1)-\frac{m(t_0)m(t_f)}{m(t_1)}\right]$$
$$\times G(t_f-t')[J(t')-J'(t)]\Bigg)\exp\left[\frac{i}{2G(T)}\left\{\frac{[m(t_0)+1]^2}{4\mathcal{A}(t)}\left[\int_{t_0}^{t_f} dt\int_{t_0}^{t_f} dt' G(t_f-t')G(t_f-t)[J'(t)J'(t')-J(t)J(t')]\right]\right. \quad (76)$$
$$\left.+2\int_{t_0}^{t_f} dt\int_{t_0}^{t_f)} dt'[\Theta(t-t')G(t_f-t)G(t'-t_0)][J'(t)J'(t')-J(t)J(t')]\right\}\Bigg].$$

Influence Phase

In the case of a Feynman path integral, the logarithm of the path integral is usually defined as the "effective action". Similarly for the Schwinger–Keldysh path integral, the logarithm of the generating function of the path integral is defined as the "influence phase". The influence phase is given by

$$\Phi = -i\ln[Z(J,J')]. \quad (77)$$

Using Equation (76), the influence phase for the inverted oscillator is given by the following expression:

$$\Phi = -i\ln\Bigg[\frac{2m(t_1)aG(T)}{\sqrt{2\pi K(t)}}\delta\Bigg(\int_{t_0}^{t_f} dt'[m(t_f)+1]\mathcal{A}(t)G(t'-t_0) + \frac{[m(t_0)+1]}{2}\left[m(t_f)+m(t_0)+m(t_1)-\frac{m(t_0)m(t_f)}{m(t_1)}\right]$$
$$\times G(t_f-t')[J(t')-J'(t)]\Bigg)\Bigg] + \frac{1}{2G(T)}\left\{\frac{[m(t_0)+1]^2}{4\mathcal{A}(t)}\left[\int_{t_0}^{t_f} dt\int_{t_0}^{t_f} dt' G(t_f-t')G(t_f-t)[J'(t)J'(t')-J(t)J(t')]\right]\right. \quad (78)$$
$$\left.+2\int_{t_0}^{t_f} dt\int_{t_0}^{t_f} dt'[\Theta(t-t')G(t_f-t)G(t'-t_0)][J'(t)J'(t')-J(t)J(t')]\right\}.$$

6. Calculation of Out-of-Time-Ordered Correlator

In this section, we compute the out-of-time-ordered correlator (OTOC) as an arbitrarily ordered 4-point correlation function for the inverted oscillator using the invariant operator method and Schwinger–Keldysh path integral formalism. Note that we closely follow the calculation of OTOCs for a harmonic oscillator [6] and modify the same for an inverted oscillator.

To do so, the invariant operator is given in Equation (12) as

$$I(t) = -\frac{1}{2}\left[\left(\frac{\hat{q}}{K(t)}\right)^2 - \left(K(t)\hat{P} - m(t)(\dot{K}(t) - f(t)K(t))\hat{q}^2\right)^2\right]. \quad (79)$$

The invariant operator given above has the form of the forced harmonic oscillator, which makes it hard to find the wavefunction $\psi(q,t)$ of the desired system. Because of this peculiar reason, it is necessary to perform the unitary transformation over the invariant operator. By doing so, the invariant operator method yields a straightforward calculation of the wavefunction.

Now, the corresponding unitary operator can be represented as

$$\hat{U} = \exp\left(-i\frac{m(t)}{K(t)}(\dot{K}(t) - f(t)K(t))\hat{q}^2\right). \quad (80)$$

If one performs the unitary transformation on the invariant operator of Equation (79), then

$$\begin{aligned}\bar{I}(t) &= U I \bar{U} \exp\left(-\tfrac{im(t)}{K(t)}(\dot{K}(t) - f(t)K(t))\hat{q}^2 \right) \\ &\times \left[-\tfrac{1}{2}\left\{ \left(\tfrac{\hat{q}}{K(t)}\right)^2 - \left(K(t)\hat{P} - m(t)(\dot{K}(t) - f(t)K(t))\hat{q}^2 \right)^2 \right\} \right] \\ &\times \exp\left(\tfrac{im(t)}{K(t)}(\dot{K}(t) - f(t)K(t))\hat{q}^2 \right) \Rightarrow \bar{I}(t) = -\tfrac{1}{2}\left[\left(\tfrac{\hat{q}(t)}{K(t)}\right)^2 - K^2(t)\hat{P}^2 \right].\end{aligned} \tag{81}$$

The new eigenstate of the invariant operator after the diagonalization will be in the below given form:

$$\begin{aligned}\varphi_n \rightarrow \bar{\varphi}_n(\hat{q}, t) &= \hat{U}\varphi_n \\ &= \exp\left(-\frac{im(t)}{K(t)}(\dot{K}(t) - f(t)K(t))\hat{q}^2 \right)\varphi_n.\end{aligned} \tag{82}$$

Then, the eigenvalue equation for the invariant operator becomes

$$\begin{aligned}\bar{I}(t)\psi_n(\hat{q}, t) &= n\psi_n(\hat{q}, t) \\ &\Rightarrow -\frac{K^2(t)}{2}\frac{\partial^2 \varphi_{(n)}}{\partial q^2} - \frac{1}{2K^2(t)}\hat{q}^2\varphi_n = n\varphi_n.\end{aligned} \tag{83}$$

The solution to Equation (83) will be in terms of the Weber function:

$$\varphi_n(\hat{q}, t) = \frac{1}{\sqrt{K(t)}} \exp\left(\frac{im(t)}{2K(t)}(\dot{K}(t) - f(t)K(t))\hat{q}^2 \right) \mathcal{D}_n\left(\sqrt{2}\,\frac{\hat{q}^2(t)}{K(t)} \right) \tag{84}$$

where $\mathcal{D}_n(x)$ is the Weber function.

Then, the expression for the eigenstate of the inverted oscillator in Equation (20) is modified in terms of the Weber function as

$$\langle q|n\rangle = \Psi(\hat{q}, t) = \frac{1}{\sqrt{K(t)}} \exp\left(-in\gamma_n(t) \right) \exp\left(\frac{im(t)}{2K(t)}(\dot{K}(t) - f(t)K(t))\hat{q}^2 \right) \mathcal{D}_n\left(\sqrt{2}\,\frac{\hat{q}^2(t)}{K(t)} \right). \tag{85}$$

Here, the phase factor is $\gamma_n(t) = \int_0^t \frac{dt'}{m(t')K^2(t')}$.

Using the form of Green's function for the inverted oscillator, computed in Appendix B, one can define the Heisenberg-picture field operator in terms of annihilation and creation operators:

$$\hat{q}(t) = \frac{\Gamma_0}{\sqrt{2}}\left(\zeta^*(t)\, a_- + \zeta(t)\, a_+ \right). \tag{86}$$

Here, $\zeta(t) = e^{\Gamma_0 t}$ and $\zeta^*(t) = e^{-\Gamma_0 t}$. Note that Γ_0 is the factor used in Green's function for the inverted oscillator given in Equation (A18). We can obtain annihilation and creation operators for inverted oscillators by putting $\omega(t) = i\omega(t)$ in the operators for any parametric oscillator [82]:

$$\begin{aligned}a_- &= \sqrt{\tfrac{i}{2}}\left[\left(\tfrac{\hat{q}}{K(t)}\right) + \left\{ K(t)\hat{P} - m(t)[\dot{K} - f(t)K(t)]\hat{q} \right\} \right] \\ a_+ &= \sqrt{\tfrac{i}{2}}\left[\left(\tfrac{\hat{q}}{K(t)}\right) - \left\{ K(t)\hat{P} - m(t)[\dot{K} - f(t)K(t)]\hat{q} \right\} \right].\end{aligned} \tag{87}$$

From this equation, we can immediately argue that $a_-^\dagger = ia_-; a_+^\dagger = ia_+$, and obviously, $[a_-, a_+] = 1$.

We can express the time evolution of the ground state of the inverted oscillator using the Heisenberg field operator, $\hat{q}(t_1)$, such that $t_1 > t_0$:

$$\begin{aligned} |\psi(t_1)\rangle &= \hat{q}(t_1)\, e^{it_0\hat{H}}\, |0\rangle \\ &= e^{it_0\hat{H}} e^{-it_0\hat{H}} \hat{q}(t_1)\, e^{it_0\hat{H}}\, |0\rangle \\ &= e^{it_0\hat{H}} \hat{q}(t_1 - t_0)\, |0\rangle\,. \end{aligned} \tag{88}$$

Similarly, one can evolve the ground state from t_1 to t_2, using a Heisenberg field operator, $\hat{q}(t_2)$, as shown below:

$$\begin{aligned} |\psi(t_2)\rangle &= \hat{q}(t_2)\, e^{it_0\hat{H}}\, |0\rangle \\ &= e^{it_1\hat{H}} e^{-it_1\hat{H}} \hat{q}(t_2)\, e^{it_0\hat{H}}\, |0\rangle \\ &= e^{it_0\hat{H}} \hat{q}(t_2 - t_1)\, |0\rangle\,. \end{aligned} \tag{89}$$

Using the form of the Heisenberg field operator in Equation (86), the time evolution in Equation (88) and Equation (89) can be expressed as

$$|\psi(t_1)\rangle = e^{it_0\hat{H}} \frac{\Gamma_0}{\sqrt{2}} \zeta(t_1 - t_0)\, |1\rangle\,, \tag{90}$$

$$|\psi(t_2)\rangle = e^{it_0\hat{H}} \frac{\Gamma_0}{\sqrt{2}} \zeta(t_2 - t_1)\, |1\rangle\,. \tag{91}$$

The two-point correlator for the ground state, $\hat{\rho} = |0\rangle\langle 0|$, of the inverted oscillator can be written as

$$\begin{aligned} Tr\left(\hat{q}(t_2)\hat{q}(t_1) e^{it_0\hat{H}}\, \hat{\rho}\, e^{-it_0\hat{H}}\right) &= \langle 0|\, e^{-it_0\hat{H}} \hat{q}(t_2)\, \hat{q}(t_1) e^{it_0\hat{H}}\, |0\rangle \\ &= \langle \psi(t_2)|\psi(t_1)\rangle. \end{aligned} \tag{92}$$

Using Equations (90) and (91), the two-point correlator for the ground state of the inverted oscillator becomes

$$Tr\left(\hat{q}(t_2)\hat{q}(t_1) e^{it_0\hat{H}}\, \hat{\rho}\, e^{-it_0\hat{H}}\right) = \frac{\Gamma_0^2}{2} \zeta(t_1 - t_0)\, \zeta^*(t_2 - t_1). \tag{93}$$

The two-point time evolution of the ground state of the inverted oscillator can be written as

$$|\psi(t_1, t_2)\rangle \equiv \hat{q}(t_2)\hat{q}(t_1) e^{i\hat{H}t_0}\, |0\rangle\,. \tag{94}$$

Using the unit operator $\hat{\mathbf{1}} = e^{i\hat{H}t_0} e^{-i\hat{H}t_0}$, remembering that $t_{1,2} > t_0$, one can rewrite the above equation as

$$\begin{aligned} |\psi(t_1, t_2)\rangle &= e^{i\hat{H}t_0} e^{-i\hat{H}t_0} \hat{q}(t_2)\hat{q}(t_1) e^{i\hat{H}t_0}\, |0\rangle \\ &= e^{i\hat{H}t_0} \hat{q}(t_2 - t_0)\hat{q}(t_1 - t_0)\, |0\rangle\,. \end{aligned} \tag{95}$$

Inserting the form of the Heisenberg field operators, from Equation (86) in Equation (95), one can show that

$$|\psi(t_1, t_2)\rangle = e^{i\hat{H}t_0} \frac{\Gamma_0}{\sqrt{2}} \zeta(t_1 - t_0) \left[\zeta^*(t_2 - t_0) a_- + \zeta(t_2 - t_0) a_+\right] |1\rangle\,. \tag{96}$$

After operating the annihilation and creation operator on $|1\rangle$, Equation (96) becomes

$$|\psi(t_1,t_2)\rangle = e^{i\hat{H}t_0}\frac{\Gamma_0}{\sqrt{2}}\zeta(t_1-t_0)\left[\zeta^*(t_2-t_0)\,|0\rangle + \sqrt{2}\zeta(t_2-t_0)\,|2\rangle\right]. \tag{97}$$

These two-point correlators can be used to compute four-point correlators. An out-of-time-ordered correlator (OTOC) [54,83] is a 4-point correlating function which can be computed without time-ordering (we can randomly take the points without considering the flow of direction of time). Equation (94) expresses the "scattering matrix" interpretation of an OTOC. If we use t_1', t_2', t_1 and t_2 instead of t_1, t_2, t_3 and t_4, then the OTOC will be

$$Tr\left(\hat{q}(t_1')\hat{q}(t_2')\hat{q}(t_2)\hat{q}(t_1)e^{i\hat{H}t_0}\,|0\rangle\,\langle 0|\,e^{-i\hat{H}t_0}\right) = \langle\psi(t_1',t_2')|\psi(t_1,t_2)\rangle. \tag{98}$$

Substituting Equation (97) in Equation (98), one can show that

$$\begin{aligned}\langle\psi(t_1',t_2')|\psi(t_1,t_2)\rangle &= \tfrac{\Gamma^2(0)}{2}\zeta(t_1-t_0)\zeta^*(t_1'-t_0)\left[\zeta(t_2'-t_0)\,\langle 0| + \sqrt{2}\zeta^*(t_2'-t_0)\,\langle 2|\right]\left[\zeta^*(t_2-t_0)\,|0\rangle + \sqrt{2}\zeta(t_2-t_0)\,|2\rangle\right]\\ &= \tfrac{\Gamma^2(0)}{2}\Big[\zeta(t_1-t_0)\zeta^*(t_1'-t_0)\zeta(t_2'-t_0)\zeta^*(t_2-t_0) + \zeta(t_1-t_0)\zeta^*(t_2'-t_0)\zeta^*(t_1'-t_0)\zeta(t_2-t_0)\\ &+\zeta(t_1-t_0)\zeta(t_2-t_0)\zeta^*(t_1'-t_0)\zeta^*(t_2'-t_0)\Big].\end{aligned} \tag{99}$$

The lesser Green's function in terms of Heisenberg field operators can be expressed as

$$G_<(t_1,t_2) = \frac{\sqrt{2}}{\Gamma_0^2}Tr\left(\hat{q}(t_2)\hat{q}(t_1)e^{i\hat{H}t_0}\hat{\rho}e^{-i\hat{H}t_0}\right). \tag{100}$$

Using the two-point correlator for the ground state of the inverted oscillator in Equation (93), we can express the lesser Green's function in the below given form:

$$G_<(t_1,t_2) = \frac{1}{\Gamma_0}\zeta(t_1-t_0)\zeta^*(t_2-t_0). \tag{101}$$

Using the results of [6], the OTOC in Equation (99) can be expressed in terms of the lesser Green's function given in Equation (101) and which is given by

$$\begin{aligned}&Tr\left(\hat{q}(t_1')\hat{q}(t_2')\hat{q}(t_2)\hat{q}(t_1)e^{i\hat{H}t_0}\,|0\rangle\,\langle 0|\,e^{-i\hat{H}t_0}\right)\\ &= \tfrac{\Gamma_0^4}{2}\Big[G_<(t_1,t_1')G_<(t_2,t_2') + G_<(t_1,t_2')G_<(t_2,t_1') + G_<(t_1,t_2)G_<(t_2',t_1')\Big].\end{aligned} \tag{102}$$

7. Numerical Results

Further explicitly writing Equation (102) by putting Green's functions from Equation (A16), one can obtain the real part of the functional form of the out-of-time-ordered correlator function: represented as

$$\mathcal{F}(t) = \left\{1 + 2e^{-f(t)t}cos\left(\frac{m_0\Omega(t)q_0^2t}{2}\right)\right\} \times \frac{1}{8}\left\{m_0^2\Omega^2(t)q_0^4 + f^2(t)\right\}. \tag{103}$$

From the above equation (Equation (103)), it is clear that the exact value of the OTOC is sensitive to the functional form of frequency and coupling of the oscillator.

In this section, using Equation (103), we numerically evaluate the exact results for OTOC measures computed by varying the functional forms of coupling, $f(t)$ and frequency, and the $\Omega(t)$ of the inverted harmonic oscillator. Particularly, we choose the coupled

$f(t)$ and frequency $\Omega(t)$ as quenched parameters and parameterize plots by varying quench protocol.

We begin by considering the mass, $m(t) = m_0 e^{\eta t}$, where m_0 is the initial mass and η is a positive and real number, which measures the rate of increment of mass. The system is very similar to the generalized Caldirola–Kanai oscillator. Since the final form of Equation (103) is independent of η, we are not very concerned about this parameter. We further set the other quantities in Equation (103) as $m_0 = 1$ and $q_0 = 10$.

- In Figure 2, we show the dynamical behavior of the OTOC, $\mathcal{F}(t)$ for similar quench protocols chosen as the coupling, $f(t) = f_0 \tanh(t)$ and frequency, $\Omega(t) = \Omega_0 \tanh(t)$ of the inverted oscillator. Here, f_0 and Ω_0 are free parameters. From all subplots, it is evident that the early-time behavior of the OTOC is characterized by fluctuating values of the OTOC such that the amplitude of these fluctuations decrease as we move further in time. We also observe that for time values on the order of magnitude 1, the OTOC values scale on the order of 10^3 or 10^4. Upon approximation, the growth exhibits an exponential behavior of the form

$$\mathcal{F}(t) = ae^{(bt)} + c$$

  with coefficients which are found, by an exponential fit of the plot, in Figure 2c to be $a = 1.73 \times 10^4$, $b = 0.442$, and $c = -1.81 \times 10^4$, all of which are non-zero. The apparent linear region near the quench can be attributed to the saturation of the exponential rise that begins after the quench point. At some time beyond the quench point $t = 1$, these oscillations are completely damped and we observe a linear rise in the value of the OTOC characterizing the chaotic nature of the system. Finally, once the dynamics of the chosen quench protocols drive the system from non-equilibrium to equilibrium, we observe that the OTOC saturates to a constant value irrespective of time. Now, one can choose different triggers to thermalize the dynamical behavior of $\mathcal{F}(t)$ by varying the value of the coupling parameter f_0. It is evident from the plots that once f_0 starts to increase, the quenched coupling triggers $\mathcal{F}(t)$ in such a way that the fluctuations tend to dampen earlier.
- Particularly in the subplot of Figure 2a, when $f_0 = 5.0$, we observe rapid oscillations having higher amplitudes in values of $\mathcal{F}(t)$ in the region $0 < t < 0.8$, marked by a red background. As we approach the quench point at $t = 1$, the amplitude of these oscillation dampens are marked by the yellow region. The chosen quench protocol then starts to thermalize the system and we observe that the fluctuations completely die out at $t \approx 1.6$. The value of $\mathcal{F}(t)$ then rises and saturates for $t > 2$. This late-time behavior of the OTOC is marked by a green background.
- In the subplot of Figure 2b, we observe a similar dynamical behavior in the value of $\mathcal{F}(t)$. However, it is evident that at the chosen value of free parameter $f_0 = 10$, the fluctuations die out at $t \approx 0.8$. Hence, the early-time behavior of the OTOC is characterized by a fluctuating vale of $\mathcal{F}(t)$ marked by a red background. This is followed by a rising value of $\mathcal{F}(t)$ for $0.8 < t < 1.2$ in the region around the quench point marked by a yellow background. Finally, beyond the quench point, the rise in the value of $\mathcal{F}(t)$ is followed by thermalization. This is marked by a green background.
- In the subplot of Figure 2c, we increase the free parameter to $f_0 = 15$. We again observe fluctuations in values of $\mathcal{F}(t)$, although dying away at $t \approx 0.5$. Most of the early-time behavior of the OTOC is characterized by fluctuations which dampen for $0 < t < 0.8$, marked by a red background. Near the quench point, in the region $0.8 < t < 1.2$, we again observe a rising behavior in value of the OTOC, marked by a yellow background. The late-time behavior evidently shows a trend of thermalization in the value of $\mathcal{F}(t)$, for the region $t > 1.2$, marked by a green background. For this parameter, we extract the quantum Lyapunov exponent by plotting the logarithm of $\mathcal{F}(t)$ with respect to time.

- The quantum Lyapunov exponent is considered as the rate of growth of the logarithmic value of the OTOC and is often used to describe the chaotic nature of the system. Using the value of the OTOC from Equation (103), we can define the Lyapunov exponent for the inverted oscillator as
$$\lambda_L = \frac{\partial}{\partial t} \log[\mathcal{F}(t)]. \tag{104}$$
One can focus on the rising trend in the $\mathcal{F}(t)$ vs. t plot, and approximate the behavior of $\mathcal{F}(t)$ in the rising region as an exponential one, $\mathcal{F}(t) \approx e^{\lambda_L t}$. λ_L can then be computed as the slope of the plot of $\log[\mathcal{F}(t)]$ vs. t.
- In Figure 3, we plot the dynamical behavior of the logarithm of the OTOC for the same parameters chosen in Figure 2c. Then, λ_L can be computed as the slope of the rising trend in this figure from $0.8 < t < 1.2$. The average slope, computed for the nearly linear region of Figure 3, was found to be $\lambda_L = 1.124$, while the average rate of change in the logarithm of $\mathcal{F}(t)$ (using Equation (104)) is $\lambda_L = 1.121$. Thus, we conclude that the extracted value of the Lyapunov exponent using the graph seems to be in agreement with that using the theoretical value. It is evident from the value of λ_L that the system of inverted oscillators is chaotic in nature.
- In Figure 4, we show the dynamical behavior of the OTOC $\mathcal{F}(t)$ for different quench protocols chosen as the coupling, $f(t) = f_0\,\mathrm{sech}(t)$ and frequency, $\Omega(t) = \Omega_0 \tanh(t)$. For all subplots, it is clear that, at early time, the value of $\mathcal{F}(t)$ fluctuates with rapid oscillations, which are dampened at some time after the quench point $t = 1$. As we move further in time, it is evident that the dynamical effects of quench protocols reduce the amplitude of $\mathcal{F}(t)$ to zero. Also, as we choose increasing values of the free parameter Ω_0, the frequency of fluctuations in the value of the OTOC increases.
- Particularly in the subplot of Figure 4a, when $\Omega_0 = 1$, we observe that the early-time behavior of $\mathcal{F}(t)$ at $0 < t < 0.8$ is dominated by fluctuations, marked by a red background. These oscillations in the value of the OTOC tend to dampen as we move further in time. Around the quench point, for $0.8 < t < 1.2$, we observe a rise, followed by a dip in the value of $\mathcal{F}(t)$, marked by a yellow background. At late time, for $t > 1.2$, the oscillations tend to die out completely, such that $\mathcal{F}(t)$ becomes zero; this is marked by a green background.
- In the subplot of Figure 4b, when we increase the free parameter as $\Omega_0 = 2.5$, we observe rapid oscillations in the value of $\mathcal{F}(t)$ with a higher frequency than that of the previous case, in the early-time region, i.e., $0 < t < 0.8$ (red background). The amplitude of these fluctuations dampens for later times. Around the quench point, $0.8 < t < 1.2$ and at late times, $t > 1.2$, we again observe a similar trend to that of the previous case, marked by a yellow and green background, respectively.
- In the subplot of Figure 4c, we further increase the free parameter, $\Omega_0 = 5$ and observe a similar trend in the dynamical behavior of $\mathcal{F}(t)$ to that of previous cases. However at early times, for $0 < t < 0.8$, the fluctuations are more rapid with a higher frequency than that of the previous case. This is marked by a red background.
- It is evident from the nature of the plots shown in Figure 2 that the similar quench protocols for coupling and frequency of the inverted oscillator trigger thermalization such that the OTOC saturates to a non-zero value at very late times. On the other hand, if we choose different quench protocols, as shown in Figure 4, for coupling and frequency of the oscillator, the OTOC, although having no fluctuation at late times, saturates to a zero value.

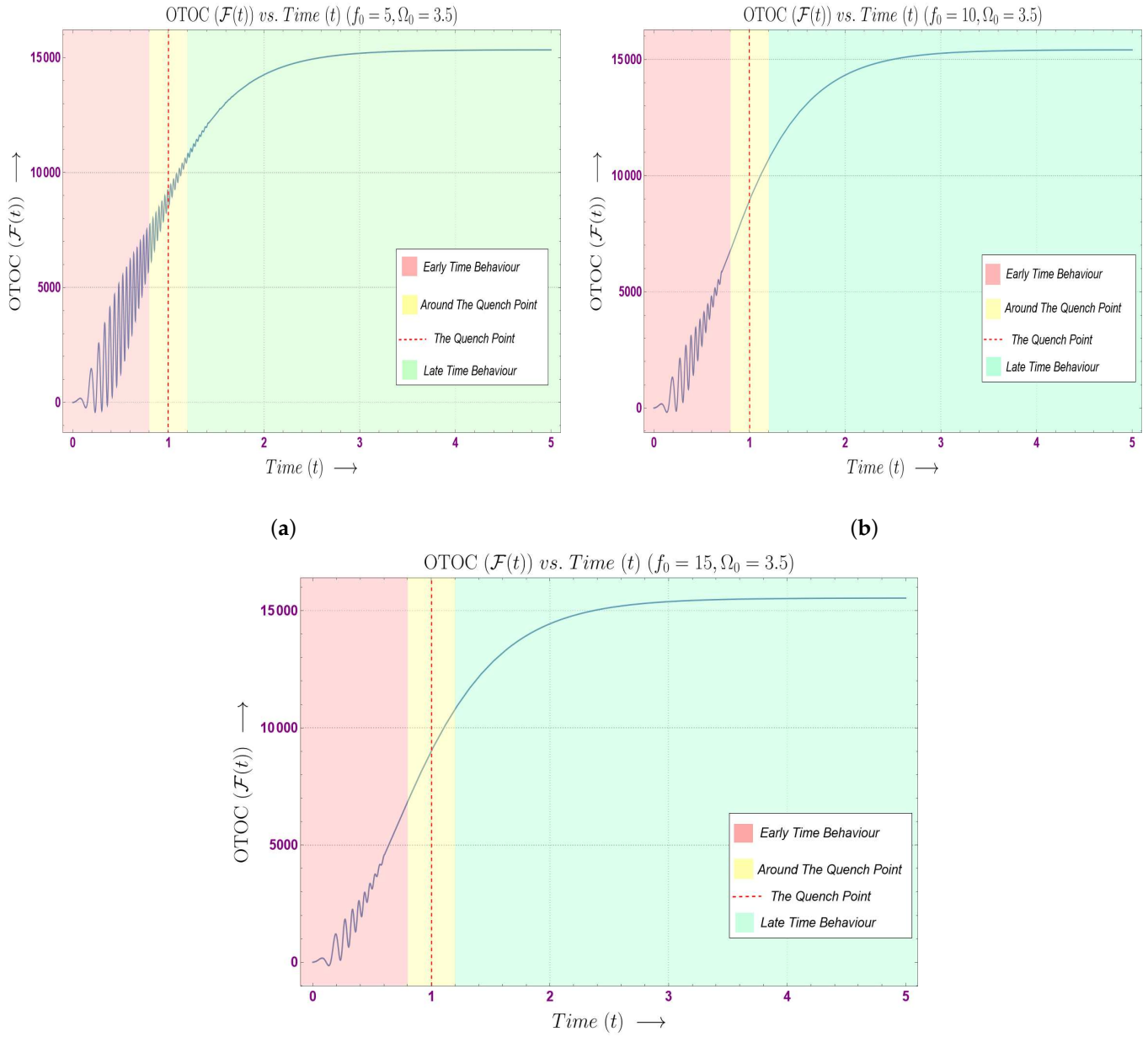

Figure 2. Variation in the OTOC $(\mathcal{F}(t))$ versus time (t) for a constant Ω_0 but different f_0, such that frequency and coupling of the inverted oscillator have the same quench profiles.

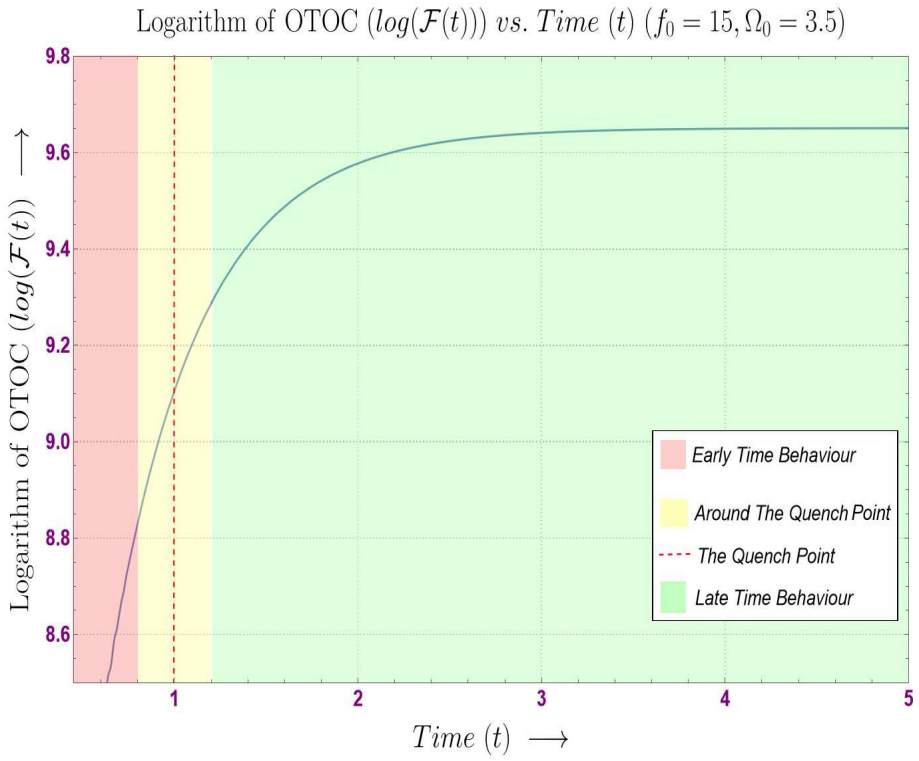

Figure 3. Variation in the logarithm of the OTOC ($\log \mathcal{F}(t)$) with respect to time (t), where we choose same quench profiles for frequency and coupling.

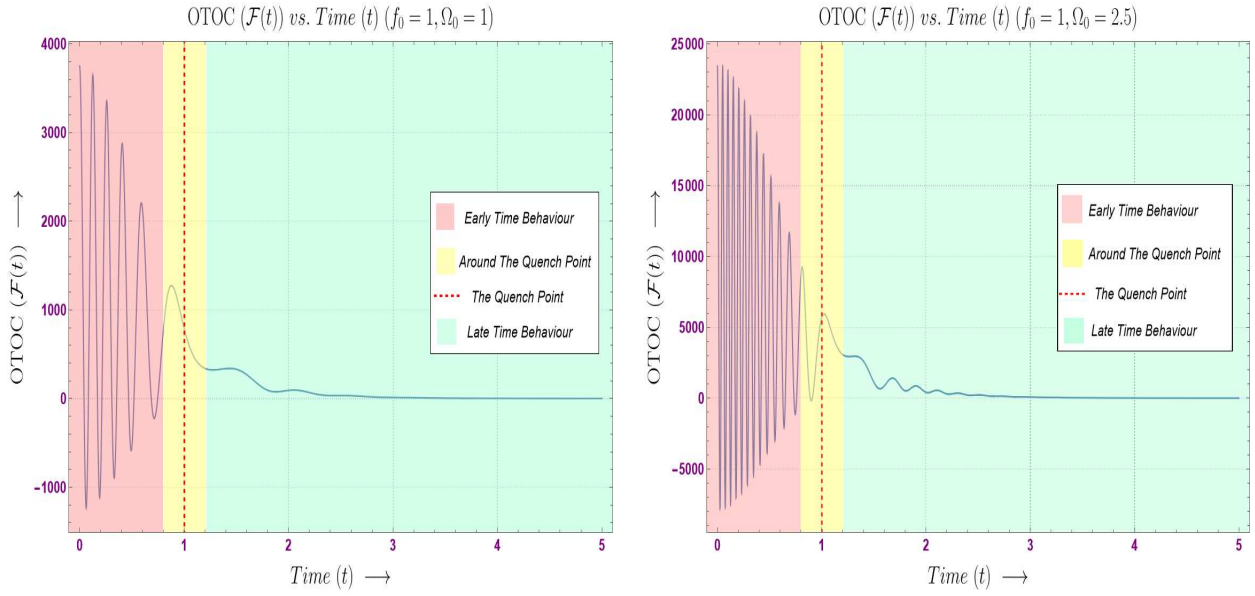

(**a**) (**b**)

Figure 4. *Cont.*

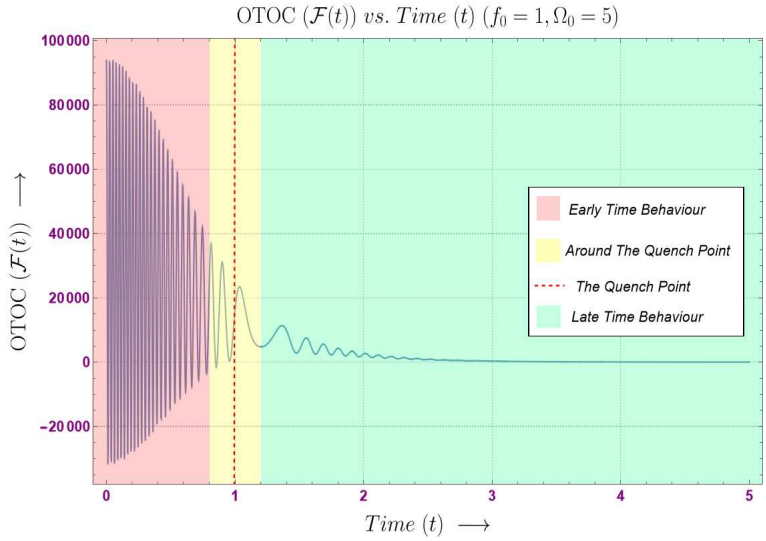

(c)

Figure 4. Variation in the OTOC $(\mathcal{F}(t))$ versus time (t) for a constant f_0 but different Ω_0, such that the frequency and coupling of the inverted oscillator have different quench profiles.

8. Conclusions

We have studied the Schwinger–Keldysh path integral formalism in the context of a generic time-dependent inverted oscillator system that is governed by non-equilibrium dynamics, with a generic Hamiltonian, and how the formalism can help to generate the out-of-time-ordered correlators (OTOCs). The following list of points serves as an epilogue for this paper:

- Starting with a time-dependent Hamiltonian of an inverted oscillator, we use the Lewis–Riesenfeld invariant method to solve the TDSE and hence compute the eigenstates and eigenvalues. We notice that these eigenvalues are independent of the state n, but are continuous functions of time. Using these eigenstates, we have derived the correlation functions in the form of a density matrix.
- Next, we calculate the time-dependent Green's function for the considered Hamiltonian of an inverted oscillator. The obtained form of Green's function is used while computing the four-point OTOC.
- Further, we derive the expression of time-dependent eigenstates of the Hamiltonian of generalized inverted oscillator in a Heisenberg picture. The two-point correlators are then derived by using the form of Green's function. It is evident that the time-dependent OTOC can be expressed in the form of the lesser Green's function.
- Next, we have expressed the classical action in terms of Heisenberg field operators and Green's functions. This action is then used to compute the generating function of the system. The final form of the generating functional is evidently dependent on Green's function and Heisenberg field operators. This generating functional is then used to evaluate the expression for the 4-point OTOC.
- Since there is no implicit time-ordering in the OTOC, one could not use Feynman path integrals to evaluate such correlators. Instead, we have employed the use of Schwinger–Keldysh path integral formalism to compute the OTOC for a time-dependent inverted oscillator. By choosing a Schwinger–Keldysh contour, we have given the exact form of OTOC for the inverted oscillator. Furthermore, we also mention the form of influence phase.
- The analytical form of the real part of the OTOC is then used to numerically evaluate the dynamical behavior of the OTOC. Furthermore, we choose quenched coupling

and frequency of the inverted oscillator, so as to comment on the thermalization of the OTOC for different parametric variations.

- From the numerical results, it is evident that there are different phases in the dynamical behavior of the OTOC, with the first being the oscillatory phase where the value of the OTOC fluctuates with a decreasing amplitude. The oscillatory phase is dominant at early times. When we set both the quenched frequency as well as coupling to the same quench protocol, then the quench seems to be thermalizing the OTOC at late time. However, before this thermalization, we observed a clear rise in the value of the OTOC, showcasing the chaotic nature of the system. We could extract the quantum Lyapunov exponent by using this rise in the value of the OTOC. Clearly, the two other phases of the OTOC are the exponential rise and saturation. Furthermore, we observe that as we increase the coupling free parameter in the chosen quench protocol, the fluctuations stop at earlier time. Hence, it can be inferred that increasing coupling essentially make the oscillatory phase of the OTOC less dominant. Also, the initial conditions when changed have drastic effects on the dynamical behavior of the OTOC, again due to the chaotic nature of the system.
- On the other hand, if we choose two different quench protocols as the quenched frequency and coupling, then at early time, the value of $\mathcal{F}(t)$ fluctuates with rapid oscillations, which are dampened at some time after the quench point $t = 1$. As there is no rise in the OTOC, one can infer that the system is no longer chaotic. As we continue to move further in time, it is evident that the dynamical effects of quench protocols through trying to thermalize the value of OTOC reduce the amplitude of $\mathcal{F}(t)$ to zero. Also, as we choose increasing values of a frequency-free parameter, the frequency of oscillations at early time increases rapidly.

Some future prospects of the present work are appended below point-wise:

- In this work, we have developed a means to compute the OTOC for an inverted oscillator in the presence of quenched parameters using its time-dependent ground state. We can develop a thermal effective field theory of this model and compute a thermal OTOC as well [6]. Inspired by the work of [84], we can then use the thermal OTOC to find that our quenched inverted oscillator model exactly saturates to the Maldacena–Shenker–Stanford (MSS) bound on the quantum *Lyapunov exponent* $\lambda \leq 2\pi/\beta$, where β represents the inverse equilibrium temperature of the representative quantum mechanical system after achieving thermalization at the late time scales. This extended version of the computation will also be extremely helpful to comment on whether maximal chaos can be achieved from the present set up or not. Studying the thermal OTOCs and scrambling time scales in systems depending on quenched inverted oscillators can be intriguing. For such a case, one needs to use the well-known *thermofield double state* [85] instead of the temperature-independent ground state to extend the present computation at finite temperature. One important assumption we need to use to explicitly perform the computation of the OTOC with the *thermofield double state* is that the system fully thermalizes at the late time scales. There are many applications in black hole physics associated with shock wave geometry [58,86–91] and in cosmology [54,92], where one can use the derived results of *Schwinger–Keldysh formalism* as well as the OTOC. However, the specific effect of the time-dependent quench in the coupling parameters of the underlying theoretical set up have not been studied yet in both the abovementioned problems. It would be really interesting to explicitly study these effects within the framework of black hole physics as well as in cosmology.
- Since in this computation, the time-dependent quantum quench plays a significant role, it is highly natural to study the thermalization phenomenon explicitly from the present set up, as we all know, quantum quench triggers the thermalization procedure in general. If the system under consideration fully thermalizes at the late time scales, then the corresponding system can be described in terms of a pure thermal ensemble and the quantum states are described by thermofield double states. But these types of

features are very special and can only happen in very specific small classes of specific theories. If we have a slow/fast quench in the coupling parameters of the theory, then it is naturally expected from the set up that before quench, just after quench, and at late time scales, the corresponding quantum mechanical states will be different. In technical language, these are pre-quench, post-quench-Calabrese–Cardy (CC), or generalized Calabrese–Cardy (gCC) [93–96] and Generalized Gibbs ensemble (if not fully thermalized) [93–96] or pure *thermofield double* states. This particular information is extremely important because the computation of an OTOC is fully dependent on the underlying quantum states. It is expected that for a given theoretical set up, we need to use three different quantum states in three different regimes to compute the expression for the OTOC in the presence of time-dependent quench in the coupling parameters of the theory. In the OTOC computation, which we have performed in this paper, we have used the ground states at zero temperature, which is technically a pre-quench state. It would be highly desirable if one could study the OTOC using the post-quench CC/gCC as well as Generalized Gibbs ensemble/thermal states. Now, one very crucial point is that which people usually do not use to construct these states at different regimes, which is the *invariant operator method*. This method allows us to construct all possible states at different time scales having a quench profile in the respective parameters of the theory. This implies that the *invariant operator method* automatically allows us to construct the corresponding quantum states in the pre-quench and post-quench regions, which is necessarily needed to compute an OTOC. Most importantly, the *invariant operator method* allows us to construct the quantum mechanical states at each instant of time in the time scale, except at the very late time scale when the full thermalization or the effective thermalization has been achieved by the underlying physical set up.

- The OTOC has been used to understand the dynamics of cosmological scalar fields [54], it would be interesting to explore such ideas in the presence of quench. Our work deals with inverted oscillators in the presence of a quench which can be applied to many models appearing in cosmology, quantum gravity, and condensed matter physics.

Author Contributions: Conceptualization, S.C.; methodology, S.C., R.M.G., S.D., S.M. and N.P.; software, R.M.G., S.D., S.M. and N.P.; validation, S.C., R.M.G., S.D., S.M. and N.P.; formal analysis, S.C., R.M.G., S.D., S.M. and N.P.; investigation, S.C.; resources, S.C.; data curation, S.C., R.M.G., S.D., S.M. and N.P.; writing—original draft preparation, S.C., R.M.G., S.D., S.M. and N.P.; writing—review and editing, S.C., R.M.G., S.D., S.M. and N.P.; visualization, S.C., R.M.G., S.D., S.M. and N.P.; supervision, S.C.; project administration, S.X.; funding acquisition, S.C. All authors have read and agreed to the published version of the manuscript.

Funding: This research received no external funding.

Data Availability Statement: The original contributions presented in the study are included in the article, further inquiries can be directed to the corresponding author.

Acknowledgments: The research work of S.C. is supported by CCSP, SGT University, Gurugram Delhi-NCR by providing the Assistant Professor (Senior Grade) position. S.C. also would like to thank CCSP, SGT University, Gurugram Delhi-NCR for providing an outstanding work-friendly environment. We would like to thank Silpadas N. from the Department of Physics, Pondicherry University for the collaboration in the initial stage of the work. S.C. would like to thank all the members of our newly formed virtual international non-profit consortium Quantum Aspects of the Space-Time and Matter (QASTM) for the elaborative discussions. Last but not least, we would like to acknowledge our debt to the people belonging to the various parts of the world for their generous and steady support of our research in natural sciences.

Conflicts of Interest: The authors declare no conflicts of interest.

Appendix A. Integration over Initial Field Configuration

In this appendix, our prime objective is to simplify the expression of the wave-function in Equation (67) by evaluating the contribution of the integral over initial field

configuration, q_0. We begin with writing the contribution of the initial field to the wave-function of inverted oscillator, $\chi(q_f|J)$ as

$$\chi(q_f|J) = \int_{-\infty}^{\infty} dq_0 \exp\left[\frac{i}{2G(T)}\left(\left[\left\{f(t_0)t_0) + \frac{i}{x_0^2}\right\}G(T) + m(t_0)\dot{G}(T) + \frac{\left[\frac{m^2(t_1)+m^2(t_0)}{m(t_1)}\right]G(t_f-t_1)}{2G(t_1-t_0)}\right]q_0^2 \right.\right.$$
$$\left.\left. -q_0\left[[m(t_f)+m(t_0)]q_f - [m(t_0)+1]\int_{t_0}^{t_f} dtG(t_f-t)J(t) + \left[m(t_1) - \frac{m(t_0)m(t_f)}{m(t_1)}\right]q_f\right]\right)\right]. \tag{A1}$$

Further, we define

$$\mathcal{A}(t) = \left[f(t_0)m(t_0) + \frac{i}{x_0^2}\right]G(T) + m(t_0)\dot{G}(T) + \frac{\left[\frac{m^2(t_1)+m^2(t_0)}{m(t_1)}\right]G(t_f-t_1)}{2G(t_1-t_0)}. \tag{A2}$$

Here,

$$\frac{1}{x_0^2} = \frac{im(t)}{2K(t)}(\dot{K}(t) - f(t)K(t)). \tag{A3}$$

Using Equation (A2), we can rewrite the expression for Equation (A1) as

$$\chi(q_f|J) = \exp\left[\frac{-i\mathcal{A}^{-1}(t)}{8G(T)}\left(\{m(t_f)+m(t_0)\}q_f - [m(t_0)+1]\int_{t_0}^{t_f} dt\, G(t_f-t)J(t) + \left[m(t_1) - \frac{m(t_0)m(t_f)}{m(t_1)}\right]q_f\right)^2\right]$$
$$\times \int_{-\infty}^{\infty} dq_0 \exp\left(\frac{i\mathcal{A}(t)}{2G(T)}[q_0-\beta]^2\right), \tag{A4}$$

where the factor β is

$$\beta = \left\{\frac{[m(t_f)+m(t_0)]q_f - [m(t_0)+1]\int t_0{}^{t_f} dt\; G(t_f-t)J(t)\left[m(t_1) - \frac{m(t_0)m(t_f)}{m(t_1)}\right]q_f}{2A(t)}\right\}. \tag{A5}$$

Then, performing the integration over q_0, one can rewrite Equation (A4) as

$$\chi(q_f|J) = \sqrt{2\pi i G(T)\mathcal{A}^{-1}(t)}\exp\left[\frac{-i\mathcal{A}^{-1}(t)}{8G(T)}\left(\left\{m(t_f)+m(t_0)+\left[m(t_1) - \frac{m(t_0)m(t_f)}{m(t_1)}\right]\right\}q_f \right.\right.$$
$$\left.\left. - (m(t_0)+1)\int_{t_0}^{t_f} dt\; G(t_f-t)J(t)\right)^2\right]. \tag{A6}$$

Since we have integrated over the initial field configuration, the generating function for the inverted oscillator is simplified and only depends on the final field configuration, q_0, as shown in Section 4.

Appendix B. Calculation of Green's Function

In this work, we have obtained the generating function and OTOC for the inverted oscillator, in terms of Green's function. We compute this Green's function for the inverted oscillator in this appendix. Although there are several time-dependent Green's functions, for our system, the most important is the outgoing or retarded Green's function. Let $U(t,t')$ be the time operator which depends on final time t' and initial time t. Since the Hamiltonian is time-dependent for our system, $U(t,t')$ will satisfy the TDSE. We can write it as

$$i\frac{\partial U(t,t')}{\partial t} = \hat{H}(t)U(t,t'). \tag{A7}$$

When we put the Hamiltonian of the inverted oscillator of Equation (1) in the above equation, we obtain

$$i\frac{\partial U(t,t')}{\partial t} = -\frac{1}{2m(t)}\frac{\partial^2 U(t,t')}{\partial q^2} - \frac{1}{2}m(t)\Omega^2(t)q^2(t)U - \frac{i}{2}f(t)U - \frac{i}{2}f(t)q(t)\frac{\partial U}{\partial q}. \quad \text{(A8)}$$

From the above equation,

$$i\frac{\partial U}{\partial t} = -\frac{1}{2}m(t)\Omega^2(t)q^2(t)U - \frac{i}{2}f(t)U. \quad \text{(A9)}$$

After multiplying the above equation by i and re-arranging, we obtain the following differential equation:

$$\frac{\partial U}{\partial t} + \left\{\frac{1}{2}f(t) - \frac{i}{2}m(t)\Omega^2(t)q^2(t)\right\}U = 0. \quad \text{(A10)}$$

The integrating factor for this differential equation will be $e^{\int\{\frac{1}{2}f(t) - \frac{i}{2}m(t)\Omega(t)q^2(t)\}dt}$. The solution of the above differential equation can be expressed using integrating factor as

$$U(t) = c\, e^{\frac{1}{2}\int\{im(t)\Omega^2(t)q^2(t) - f(t)\}dt}. \quad \text{(A11)}$$

Here, c is a real constant. In quantum mechanics, the outgoing or retarded Green's Function is defined by

$$G_+(q,t;q',t') = \Theta(t-t')\,\langle q|\,U(t,t')\,|q'\rangle\,, \quad \text{(A12)}$$

and the incoming or advanced Green's function is

$$G_-(q,t;q',t') = \Theta(t'-t)\,\langle q|\,U(t,t')\,|q'\rangle\,. \quad \text{(A13)}$$

The combined form of Green's function using Equation (A11) can be given as

$$\begin{aligned}\hat{G}_\pm &= \pm\Theta\Big(\pm(t-t')\Big)U(t,t') \\ &= \pm\Theta\Big(\pm(t-t')\Big)c\, e^{\frac{1}{2}\int\{im(t)\Omega^2(t)q^2(t) - f(t)\}dt}. \end{aligned} \quad \text{(A14)}$$

In the above equation, we can eliminate the integration from the power of the exponential by assuming

$$\frac{d(\Gamma(t)t)}{dt} = \frac{1}{2}(im(t)\Omega^2(t)q^2(t) - f(t)). \quad \text{(A15)}$$

Using Equation (A15), one can rewrite Green's function in Equation (A14) as

$$G(t) = c\, e^{\int \frac{d(\Gamma(t)t)}{dt}\,dt} = c\, e^{\Gamma(t)t}. \quad \text{(A16)}$$

To apply the boundary condition, we need to change Equation (A16) in terms of hyperbolic sines and cosines, as given below:

$$G(t) = A\,\sinh(\Gamma(t)t) + B\,\cosh(\Gamma(t)t). \quad \text{(A17)}$$

Applying the boundary conditions $G(0) = 0$ and $\dot{G}(0) = 1$, Green's function for the inverted oscillator is

$$G(t) = \frac{1}{\Gamma_0}\,\sinh\Big(\Gamma(t)t\Big). \quad \text{(A18)}$$

References

1. Schwinger, J. Brownian Motion of a Quantum Oscillator. *J. Math. Phys.* **1961**, *2*, 407–432. [CrossRef]
2. Keldysh, L.V. Diagram technique for nonequilibrium processes. *Sov. Phys. JETP* **1965**, *20*, 1018–1026.
3. Haehl, F.M.; Loganayagam, R.; Rangamani, M. Schwinger-Keldysh formalism. Part I: BRST symmetries and superspace. *JHEP* **2017**, *6*, 069. [CrossRef]
4. Haehl, F.M.; Loganayagam, R.; Rangamani, M. Schwinger-Keldysh formalism. Part II: Thermal equivariant cohomology. *JHEP* **2017**, *6*, 070. [CrossRef]
5. Geracie, M.; Haehl, F.M.; Loganayagam, R.; Narayan, P.; Ramirez, D.M.; Rangamani, M. Schwinger-Keldysh superspace in quantum mechanics. *Phys. Rev. D* **2018**, *97*, 105023. [CrossRef]
6. BenTov, Y. Schwinger-Keldysh path integral for the quantum harmonic oscillator *arXiv* **2021**, arXiv:2102.05029. [CrossRef]
7. Bohra, H.; Choudhury, S.; Chauhan, P.; Narayan, P.; Panda, S.; Swain, A. Relating the curvature of De Sitter Universe to Open Quantum Lamb Shift Spectroscopy. *arXiv* **2019**, arXiv:1905.07403. [CrossRef]
8. Sieberer, L.M.; Chiocchetta, A.; Gambassi, A.; Täuber, U.C.; Diehl, S. Thermodynamic Equilibrium as a Symmetry of the Schwinger-Keldysh Action. *Phys. Rev. B* **2015**, *92*, 134307. [CrossRef]
9. Georgii, H.O. *Gibbs Measures and Phase Transitions*; De Gruyter: Berlin, Germany; New York, NY, USA, 2011. [CrossRef]
10. Takahashi, Y. On the generalized ward identity. *Nuovo C.* **1957**, *6*, 371–375. [CrossRef]
11. Peskin, M.; Schroeder, D. *An Introduction to Quantum Field Theory*; Westview Press: Boulder, CO, USA, 1995.
12. Choudhury, S.; Mukherjee, A.; Chauhan, P.; Bhattacherjee, S. Quantum Out-of-Equilibrium Cosmology. *Eur. Phys. J. C* **2019**, *79*, 320. [CrossRef]
13. Akhtar, S.; Choudhury, S.; Chowdhury, S.; Goswami, D.; Panda, S.; Swain, A. Open Quantum Entanglement: A study of two atomic system in static patch of de Sitter space. *Eur. Phys. J. C* **2020**, *80*, 748. [CrossRef]
14. Chen, X.; Wang, Y.; Xianyu, Z.Z. Schwinger-Keldysh Diagrammatics for Primordial Perturbations. *JCAP* **2017**, *12*, e006. [CrossRef]
15. Boyanovsky, D.; de Vega, H.J.; Holman, R. Nonequilibrium evolution of scalar fields in FRW cosmologies I. *Phys. Rev. D* **1994**, *49*, 2769–2785. [CrossRef]
16. Glorioso, P.; Crossley, M.; Liu, H. A prescription for holographic Schwinger-Keldysh contour in non-equilibrium systems. *arXiv* **2018**, arXiv:1812.08785. http://arxiv.org/abs/1812.08785.
17. Haehl, F.M.; Loganayagam, R.; Rangamani, M. The Fluid Manifesto: Emergent symmetries, hydrodynamics, and black holes. *JHEP* **2016**, *1*, 184. [CrossRef]
18. Herzog, C.P.; Son, D.T. Schwinger-Keldysh propagators from AdS/CFT correspondence. *JHEP* **2003**, *3*, e046. [CrossRef]
19. Giecold, G.C. Fermionic Schwinger-Keldysh Propagators from AdS/CFT. *JHEP* **2009**, *10*, 057. [CrossRef]
20. Choudhury, S.; Panda, S. Entangled de Sitter from stringy axionic Bell pair I: An analysis using Bunch–Davies vacuum. *Eur. Phys. J. C* **2018**, *78*, 52. [CrossRef]
21. Choudhury, S.; Panda, S. Quantum entanglement in de Sitter space from stringy axion: An analysis using α vacua. *Nucl. Phys. B* **2019**, *943*, 114606. [CrossRef]
22. Choudhury, S.; Gharat, R.M.; Mandal, S.; Pandey, N.; Roy, A.; Sarker, P. Entanglement in interacting quenched two-body coupled oscillator system. *Phys. Rev. D* **2022**, *106*, 025002. [CrossRef]
23. Lewis, H.R.; Riesenfeld, W.B. An Exact Quantum Theory of the Time-Dependent Harmonic Oscillator and of a Charged Particle in a Time-Dependent Electromagnetic Field. *J. Math. Phys.* **1969**, *10*, 1458–1473. [CrossRef]
24. Andrzejewski, K. Dynamics of entropy and information of time-dependent quantum systems: Exact results. *Quant. Inf. Proc.* **2022**, *21*, 117. [CrossRef]
25. Khantoul, B.; Bounames, A.; Maamache, M. On the invariant method for the time-dependent non-Hermitian Hamiltonians. *Eur. Phys. J. Plus* **2017**, *132*, 258. [CrossRef]
26. Choudhury, S. Cosmological Geometric Phase From Pure Quantum States: A study without/with having Bell's inequality violation. *arXiv* **2021**, arXiv:2105.06254. [CrossRef]
27. Choi, J.R. Coherent and squeezed states for light in homogeneous conducting linear media by an invariant operator method. *Int. J. Theor. Phys.* **2004**, *43*, 2113–2136. [CrossRef]
28. Kanasugi, H.; Okada, H. Systematic Treatment of General Time-Dependent Harmonic Oscillator in Classical and Quantum Mechanics. *Prog. Theor. Phys.* **1995**, *93*, 949–960. [CrossRef]
29. Choudhury, S.; Pal, S. Fourth level MSSM inflation from new flat directions. *JCAP* **2012**, *4*, 018. [CrossRef]
30. Choudhury, S.; Pal, S. DBI Galileon inflation in background SUGRA. *Nucl. Phys. B* **2013**, *874*, 85–114. [CrossRef]
31. Choudhury, S.; Pal, S. Brane inflation in background supergravity. *Phys. Rev. D* **2012**, *85*, 043529. [CrossRef]
32. Choudhury, S.; Chakraborty, T.; Pal, S. Higgs inflation from new Kähler potential. *Nucl. Phys. B* **2014**, *880*, 155–174. [CrossRef]
33. Choudhury, S.; Panda, S. COSMOS-e'-GTachyon from string theory. *Eur. Phys. J. C* **2016**, *76*, 278. [CrossRef]
34. Bhattacharyya, A.; Das, S.; Haque, S.S.; Underwood, B. Rise of cosmological complexity: Saturation of growth and chaos. *Phys. Rev. Res.* **2020**, *2*, 033273. [CrossRef]
35. Choudhury, S. COSMOS-e'-Soft Higgsotic attractors. *Eur. Phys. J. C* **2017**, *77*, 469. [CrossRef]
36. Choudhury, S.; Panda, S.; Singh, R. Bell violation in primordial cosmology. *Universe* **2017**, *3*, 13. [CrossRef]
37. Choudhury, S.; Panda, S.; Singh, R. Bell violation in the Sky. *Eur. Phys. J. C* **2017**, *77*, 60. [CrossRef]

38. Ali, T.; Bhattacharyya, A.; Haque, S.S.; Kim, E.H.; Moynihan, N.; Murugan, J. Chaos and Complexity in Quantum Mechanics. *Phys. Rev. D* **2020**, *101*, 026021. [CrossRef]
39. Bhattacharyya, A.; Das, S.; Shajidul Haque, S.; Underwood, B. Cosmological Complexity. *Phys. Rev. D* **2020**, *101*, 106020. [CrossRef]
40. Einhorn, M.B.; Larsen, F. Squeezed states in the de Sitter vacuum. *Phys. Rev. D* **2003**, *68*, 064002. [CrossRef]
41. Grain, J.; Vennin, V. Canonical transformations and squeezing formalism in cosmology. *JCAP* **2020**, *2*, e022. [CrossRef]
42. Grishchuk, L.; Haus, H.A.; Bergman, K. Generation of squeezed radiation from vacuum in the cosmos and the laboratory. *Phys. Rev. D* **1992**, *46*, 1440–1449. [CrossRef]
43. Bhargava, P.; Choudhury, S.; Chowdhury, S.; Mishara, A.; Selvam, S.P.; Panda, S.; Pasquino, G.D. Quantum aspects of chaos and complexity from bouncing cosmology: A study with two-mode single field squeezed state formalism. *SciPost Phys. Core* **2021**, *4*, e026. [CrossRef]
44. Choudhury, S.; Chowdhury, S.; Gupta, N.; Mishara, A.; Selvam, S.P.; Panda, S.; Pasquino, G.D.; Singha, C.; Swain, A. Circuit Complexity From Cosmological Islands. *Symmetry* **2021**, *13*, 1301. [CrossRef]
45. Adhikari, K.; Choudhury, S.; Chowdhury, S.; Shirish, K.; Swain, A. Circuit complexity as a novel probe of quantum entanglement: A study with black hole gas in arbitrary dimensions. *Phys. Rev. D* **2021**, *104*, 065002. [CrossRef]
46. Choudhury, S.; Mukherjee, A.; Pandey, N.; Roy, A. Causality Constraint on Circuit Complexity from $\mathcal{COSMOEFT}$. *arXiv* **2021**, arXiv:2111.11468. [CrossRef]
47. Martin, J.; Vennin, V. Real-space entanglement in the Cosmic Microwave Background. *J. Cosmol. Astropart. Phys.* **2021**, *2021*, e036. [CrossRef]
48. Choudhury, S.; Panda, S.; Pandey, N.; Roy, A. Four-mode squeezed states in de Sitter space: A study with two field interacting quantum system. *Prog. Phys.* **2022**, *70*, e036. [CrossRef]
49. Heyl, M.; Pollmann, F.; Dóra, B. Detecting Equilibrium and Dynamical Quantum Phase Transitions in Ising Chains via Out-of-Time-Ordered Correlators. *Phys. Rev. Lett.* **2018**, *121*, 016801. [CrossRef]
50. Chaudhuri, S.; Loganayagam, R. Probing out-of-time-order correlators. *J. High Energy Phys.* **2019**, *2019*, 6. [CrossRef]
51. Haehl, F.M.; Loganayagam, R.; Narayan, P.; Nizami, A.A.; Rangamani, M. Thermal out-of-time-order correlators, KMS relations, and spectral functions. *J. High Energy Phys.* **2017**, *2017*, 154. [CrossRef]
52. Chakrabarty, B.; Chaudhuri, S.; Loganayagam, R. Out of time ordered quantum dissipation. *J. High Energy Phys.* **2019**, *2019*, 102. [CrossRef]
53. Chaudhuri, S.; Chowdhury, C.; Loganayagam, R. Spectral representation of thermal OTO correlators. *J. High Energy Phys.* **2019**, *2019*, 18. [CrossRef]
54. Choudhury, S. The Cosmological OTOC: Formulating new cosmological micro-canonical correlation functions for random chaotic fluctuations in Out-of-Equilibrium Quantum Statistical Field Theory. *Symmetry* **2020**, *12*, 1527. [CrossRef]
55. Hashimoto, K.; Murata, K.; Yoshii, R. Out-of-time-order correlators in quantum mechanics. *J. High Energy Phys.* **2017**, *2017*, 138. [CrossRef]
56. Haehl, F.M.; Loganayagam, R.; Narayan, P.; Rangamani, M. Classification of out-of-time-order correlators. *arXiv* **2017**, arXiv:1701.02820. [CrossRef]
57. Chakrabarty, B.; Chaudhuri, S. Out of time ordered effective dynamics of a quartic oscillator. *SciPost Phys.* **2019**, *7*, 013. [CrossRef]
58. Shenker, S.H.; Stanford, D. Black holes and the butterfly effect. *JHEP* **2014**, *3*, 067. [CrossRef]
59. Kitaev, A.; Suh, S.J. The soft mode in the Sachdev-Ye-Kitaev model and its gravity dual. *JHEP* **2018**, *5*, 183. [CrossRef]
60. Larkin, A.I.; Ovchinnikov, Y.N. Quasiclassical Method in the Theory of Superconductivity. *Sov. J. Exp. Theor. Phys.* **1969**, *28*, 1200.
61. Dray, T.; Hooft, G. The gravitational shock wave of a massless particle. *Nucl. Phys. B* **1985**, *253*, 173–188. [CrossRef]
62. 't Hooft, G. The black hole interpretation of string theory. *Nucl. Phys. B* **1990**, *335*, 138–154. [CrossRef]
63. Polkovnikov, A.; Sengupta, K.; Silva, A.; Vengalattore, M. Colloquium: Nonequilibrium dynamics of closed interacting quantum systems. *Rev. Mod. Phys.* **2011**, *83*, 863–883. [CrossRef]
64. Gogolin, C.; Eisert, J. Equilibration, thermalisation, and the emergence of statistical mechanics in closed quantum systems. *Rep. Prog. Phys.* **2016**, *79*, 056001. [CrossRef] [PubMed]
65. Calabrese, P.; Essler, F.H.L.; Mussardo, G. Introduction to 'Quantum Integrability in Out of Equilibrium Systems'. *J. Stat. Mech. Theory Exp.* **2016**, *2016*, 064001. [CrossRef]
66. Langen, T.; Gasenzer, T.; Schmiedmayer, J. Prethermalization and universal dynamics in near-integrable quantum systems. *J. Stat. Mech. Theory Exp.* **2016**, *2016*, 064009. [CrossRef]
67. Kinoshita, T.; Wenger, T.; Weiss, D. A quantum Newton's cradle. *Nature* **2006**, *440*, 900–903. [CrossRef] [PubMed]
68. Hofferberth, S.; Lesanovsky, I.; Fischer, B.; Schumm, T.; Schmiedmayer, J. Non-equilibrium coherence dynamics in one-dimensional Bose gases. *Nature* **2007**, *449*, 324–327. [CrossRef]
69. Trotzky, S.; Chen, Y.A.; Flesch, A.; McCulloch, I.P.; Schollwöck, U.; Eisert, J.; Bloch, I. Probing the relaxation towards equilibrium in an isolated strongly correlated one-dimensional Bose gas. *Nat. Phys.* **2012**, *8*, 325–330. [CrossRef]
70. Gring, M.; Kuhnert, M.; Langen, T.; Kitagawa, T.; Rauer, B.; Schreitl, M.; Mazets, I.; Smith, D.A.; Demler, E.; Schmiedmayer, J. Relaxation and Prethermalization in an Isolated Quantum System. *Science* **2012**, *337*, 1318–1322. [CrossRef]
71. Cheneau, M.; Barmettler, P.; Poletti, D.; Endres, M.; Schauß, P.; Fukuhara, T.; Gross, C.; Bloch, I.; Kollath, C.; Kuhr, S. Light-cone-like spreading of correlations in a quantum many-body system. *Nature* **2012**, *481*, 484–487. [CrossRef]

72. Meinert, F.; Mark, M.J.; Kirilov, E.; Lauber, K.; Weinmann, P.; Daley, A.J.; Nägerl, H.C. Quantum Quench in an Atomic One-Dimensional Ising Chain. *Phys. Rev. Lett.* **2013**, *111*, 053003. [CrossRef]
73. Langen, T.; Geiger, R.; Kuhnert, M.; Rauer, B.; Schmiedmayer, J. Local emergence of thermal correlations in an isolated quantum many-body system. *Nat. Phys.* **2013**, *9*, 640–643. [CrossRef]
74. Fukuhara, T.; Schauß, P.; Endres, M.; Hild, S.; Cheneau, M.; Bloch, I.; Gross, C. Microscopic observation of magnon bound states and their dynamics. *Nature* **2013**, *502*, 76–79. [CrossRef] [PubMed]
75. Fukuhara, T.; Kantian, A.; Endres, M.; Cheneau, M.; Schauß, P.; Hild, S.; Bellem, D.; Schollwöck, U.; Giamarchi, T.; Gross, C.; et al. Quantum dynamics of a mobile spin impurity. *Nat. Phys.* **2013**, *9*, 235–241. [CrossRef]
76. Borgonovi, F.; Izrailev, F.M.; Santos, L.F. Timescales in the quench dynamics of many-body quantum systems: Participation ratio versus out-of-time ordered correlator. *Phys. Rev. E* **2019**, *99*, 052143. [CrossRef]
77. Torres-Herrera, E.J.; García-García, A.M.; Santos, L.F. Generic dynamical features of quenched interacting quantum systems: Survival probability, density imbalance, and out-of-time-ordered correlator. *Phys. Rev. B* **2018**, *97*, 060303. [CrossRef]
78. Fan, R.; Zhang, P.; Shen, H.; Zhai, H. Out-of-time-order correlation for many-body localization. *Sci. Bull.* **2017**, *62*, 707–711. [CrossRef]
79. Ghosh, S.; Gupta, K.S.; Srivastava, S.C.L. Exact relaxation dynamics and quantum information scrambling in multiply quenched harmonic chains. *Phys. Rev. E* **2019**, *100*, 012215. [CrossRef]
80. Dağ, C.B.; Sun, K. Dynamical crossover in the transient quench dynamics of short-range transverse-field Ising models. *Phys. Rev. B* **2021**, *103*, 214402. [CrossRef]
81. Pedrosa, I.; de Lima, A.L.; de M. Carvalho, A.M. Gaussian wave packet states of a generalized inverted harmonic oscillator with time-dependent mass and frequency. *Can. J. Phys.* **2015**, *93*, 841–845. [CrossRef]
82. Rajeev, K.; Chakraborty, S.; Padmanabhan, T. Inverting a normal harmonic oscillator: Physical interpretation and applications. *Gen. Rel. Grav.* **2018**, *50*, 116. [CrossRef]
83. Bhagat, K.Y.; Bose, B.; Choudhury, S.; Chowdhury, S.; Das, R.N.; Dastider, S.G.; Gupta, N.; Maji, A.; Pasquino, G.D.; Paul, S. The Generalized OTOC from Supersymmetric Quantum Mechanics—Study of Random Fluctuations from Eigenstate Representation of Correlation Functions. *Symmetry* **2020**, *13*, 44. [CrossRef]
84. Maldacena, J.; Shenker, S.H.; Stanford, D. A bound on chaos. *JHEP* **2016**, *8*, 106. [CrossRef]
85. Cottrell, W.; Freivogel, B.; Hofman, D.M.; Lokhande, S.F. How to Build the Thermofield Double State. *JHEP* **2019**, *2*, 058. [CrossRef]
86. Shenker, S.H.; Stanford, D. Stringy effects in scrambling. *JHEP* **2015**, *5*, 132. [CrossRef]
87. Roberts, D.A.; Stanford, D.; Susskind, L. Localized shocks. *JHEP* **2015**, *3*, 051. [CrossRef]
88. Roberts, D.A.; Stanford, D. Two-dimensional conformal field theory and the butterfly effect. *Phys. Rev. Lett.* **2015**, *115*, 131603. [CrossRef]
89. Stanford, D.; Susskind, L. Complexity and Shock Wave Geometries. *Phys. Rev. D* **2014**, *90*, 126007. [CrossRef]
90. Stanford, D. Black Holes and the Butterfly Effect. Ph.D. Thesis. Stanford University, Stanford, CA, USA, 2014.
91. Shenker, S.H.; Stanford, D. Multiple Shocks. *JHEP* **2014**, *12*, 046. [CrossRef]
92. Choudhury, S. The Cosmological OTOC: A New Proposal for Quantifying Auto-correlated Random Non-chaotic Primordial Fluctuations. *Symmetry* **2021**, *13*, 599. [CrossRef]
93. Banerjee, P.; Gaikwad, A.; Kaushal, A.; Mandal, G. Quantum quench and thermalization to GGE in arbitrary dimensions and the odd-even effect. *JHEP* **2020**, *9*, 027. [CrossRef]
94. Mandal, G.; Paranjape, S.; Sorokhaibam, N. Thermalization in 2D critical quench and UV/IR mixing. *JHEP* **2018**, *1*, e027. [CrossRef]
95. Paranjape, S.; Sorokhaibam, N. Exact Growth of Entanglement and Dynamical Phase Transition in Global Fermionic Quench. *arXiv* **2016**, arXiv:1609.02926. [CrossRef]
96. Banerjee, S.; Choudhury, S.; Chowdhury, S.; Knaute, J.; Panda, S.; Shirish, K. Thermalization in Quenched De Sitter Space. *arXiv* **2021**, arXiv:2104.10692. [CrossRef]